New Journal of Physics
The open–access journal for physics

Nearly spherical vesicles in an external flow

V V Lebedev[1], K S Turitsyn[1,2] and S S Vergeles[1]

[1] Landau Institute for Theoretical Physics, Moscow, Kosygina 2, 119334, Russia
[2] James Franck Institute, University of Chicago, Chicago, IL 60637, USA
E-mail: turitsyn@uchicago.edu

New Journal of Physics **10** (2008) 043044 (35pp)
Received 20 December 2007
Published 24 April 2008
Online at http://www.njp.org/
doi:10.1088/1367-2630/10/4/043044

Abstract. We theoretically analyze a vesicle with small excess area, which is immersed in an external flow. A dynamical equation for the vesicle evolution is obtained by solving the Stokes equation with suitable boundary conditions imposed on the membrane. The equation has solutions corresponding to different types of motion, such as tank-treading, tumbling and trembling. A phase diagram reflecting the regimes is constructed in terms of two dimensionless parameters that depend on the vesicle excess area, the fluid viscosities, the membrane viscosity and bending modulus, the strength of the flow, and the ratio of the elongational and rotational components of the flow. We investigate the peculiarities of the vesicle dynamics near the tank-treading to tumbling and the tank-treading to trembling transitions, which occur via a saddle–node bifurcation and a Hopf bifurcation, respectively. We examine the slowdown of the vesicle dynamics near the merging point and also predict the existence of a novel dynamic regime, which we call spinning.

Contents

1. Introduction **2**
2. Basic relations **4**
2.1. Vesicle description . . . 4
2.2. Flow near the vesicle . . . 5
2.3. Membrane stress . . . 6
2.4. Membrane shape parametrization . . . 8
3. Weak flows **8**
3.1. Perturbation expansion . . . 8
3.2. Equilibrium . . . 9
3.3. Weak external flow, phenomenology . . . 11
4. General dynamic equation **12**
4.1. Closed equation . . . 12
4.2. Second-order angular harmonic . . . 14
4.3. Rescaled equation . . . 15
5. Planar external flow **16**
5.1. General consideration . . . 17
5.2. Symmetric solution . . . 18
5.3. Spinning . . . 19
6. Phase diagram of the system **20**
6.1. The tank-treading to trembling transition . . . 20
6.2. The tank-treading to tumbling transition . . . 22
6.3. Complete phase diagram . . . 24
7. Special cases **26**
7.1. Almost rotational flows and big viscosity contrast . . . 26
7.2. Purely elongational flow . . . 27
7.3. Weak external flows . . . 28
8. Strong external flows **29**
8.1. Truncated equations . . . 29
8.2. Slow dynamics . . . 30
8.3. Extremely strong flows . . . 31
9. Conclusion **32**
Acknowledgments **34**
References **34**

1. Introduction

The dynamics of soft deformable objects in external flows has been a subject of great attention recently. Experiments show that biological cells, microcapsules and vesicles exhibit several different types of motion when immersed in a flowing liquid [1]–[7]. For instance three types of dynamical behaviors were observed in experiments on vesicles in shear flow. In the tank-treading regime the vesicle shape is stationary, while the membrane rotates. The tumbling regime corresponds to the periodic flipping of the vesicle in the shear plane. The trembling

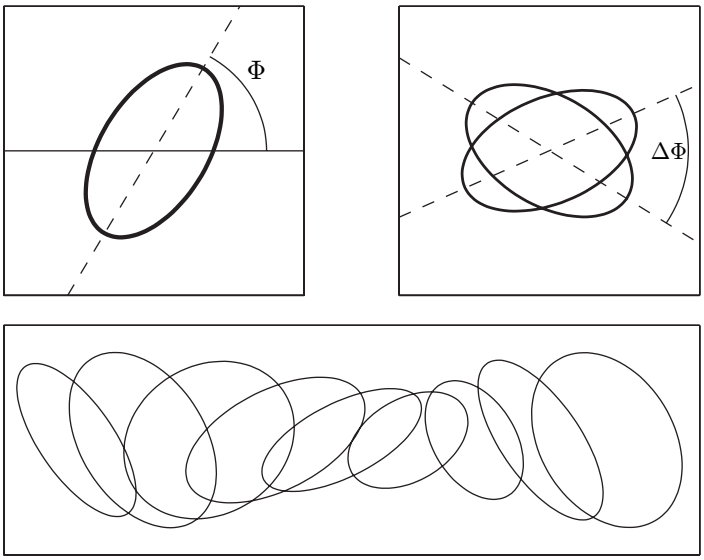

Figure 1. Vesicle projections to the shear plane in the tank-treading, trembling and tumbling regimes.

motion, experimentally discovered in the work [7], is an intermediate regime between tank-treading and tumbling, where the vesicle trembles around the direction of the flow. This regime has also been discussed in theoretical works under the names of 'vacillating–breathing' [8] and 'swinging' [9]. Different types of vesicle motion are schematically shown in figure 1.

Theoretical description of the vesicle dynamics has proved to be a challenging and complicated problem, mainly due to the nonlinear and non-local nature of the equations describing the vesicle evolution. Different strategies have been proposed to approach this problem. Numerical simulations of vesicles have been based on a variety of computational methods that include boundary element methods [10, 11], mesoscopic particle-based approximations [12]–[16] and advected field approaches [17]–[20]. While these simulations improved the understanding of vesicle dynamics, they did not completely predict the type of vesicle motion for a given set of physical parameters. Analytical studies of vesicle dynamics have been either based on extensions of the phenomenological model proposed by Keller and Skallak [21], see [9, 13, 22], or devoted to an analysis of the particular case of nearly spherical (quasi-spherical) vesicles where one can apply perturbative techniques [8], [23]–[25]. The latter approach has proved itself as one of the most efficient as long as it allowed mathematically rigorous analysis of this complex problem.

In this paper, we present a systematic study of the dynamics of nearly spherical (quasi-spherical) vesicles in aqueous solutions. We consider a quite general situation where the membrane is a viscous two-dimensional fluid, the fluids surrounding the membrane have different viscosities and the external flow can be arbitrary but planar. In this case we show that, as parameters such as viscosity ratios and external velocity gradient are varied, all three types of experimentally observed dynamic behaviors can occur. We construct the corresponding phase diagram and identify two types of bifurcations that describe the transitions between the tank-treading to tumbling and the tank-treading to trembling regimes. We analyze the 'critical' slowdown of the dynamics near the transition lines and in the vicinity of their merging point.

Some of the results derived in this paper were already reported in [26]. Here, we present significantly more detailed derivations and analyze several aspects of the problem that were not addressed in [26]. In particular, we discuss a new regime of the vesicle dynamics in an external flow: spinning, which can be observed at relatively large values of the velocity gradient and viscosity contrast.

Recently, the paper [27] was published where a theoretical scheme similar to our approach is developed. Dankel *et al* [27] reproduced our equations for the vesicle dynamics published in [26] and included some additional terms. We discuss their importance in the body of our paper and summarize our arguments concerning these terms in the conclusion section.

The structure of our paper is as follows. In section 2, we review basic theoretical facts concerning the physics of membranes. Special attention is given to the dynamic properties of membranes which can be treated as moving interfaces immersed in a 3*d* fluid. In section 3, we discuss the features of nearly spherical vesicles, analyze their equilibrium properties, and derive a phenomenological equation describing their dynamics in weak external flows. In section 4, we derive a dynamic equation for the vesicle evolution by expanding over the small deviations of the vesicle shape from the ideal sphere and the dimensionless parameters controlling the vesicle behavior are introduced. In section 5, we restrict our study to planar external velocity fields. In this case it is possible to find solutions of the dynamic equations corresponding to tank-treading, trembling, tumbling and spinning. In section 6, we examine the phase diagram of the system. We analyze the bifurcations corresponding to the tank-treading to tumbling and to the tank-treading to trembling transitions, and we describe a 'critical' slowdown of the dynamics near the merging point of the transition lines. In section 7, we study some special cases, in particular a purely elongational and nearly rotational flow. We also derive an expression for the phenomenological constant describing the vesicle dynamics in weak flows. In section 8, we investigate in detail the case of strong external flows. Finally, in section 9, we discuss some outcomes of our work and its possible extensions.

2. Basic relations

We start by reviewing the basic theory of vesicles formed by lipid bilayer membranes. The physics of membranes has been extensively studied in the past three decades. The main results on this subject can be found in [28]–[34]. Here, we consider the simplest types of membranes that are lipid bilayers. These membranes are usually used in hydrodynamic vesicle experiments. We expose principal theoretical facts concerning the membrane elasticity, which are later used in the formulation of the dynamic equations describing the vesicle dynamics. We take into account both the membrane bending elasticity and its internal viscosity, which can be relevant near the main phase transition point in membranes [35].

2.1. Vesicle description

We are interested in the processes that take place on scales of the order of the vesicle size, which is assumed to be much larger than the membrane thickness. This assumption is well justified for giant vesicles, which are usually used in experiments. In this case, in the main approximation, the membrane can be considered as infinitesimally thin, that is, as a 2*d* object (film) immersed in a 3*d* fluid. Then the vesicle is characterized solely by its geometrical shape. In other words,

in this limit the vesicle membrane can be regarded as an interface separating different pieces of the fluid.

We assume that the vesicle membrane is incompressible and impermeable to the fluid. These two properties imply that both the vesicle volume $\mathcal{V}$ and its surface area $\mathcal{A}$ are conserved, provided the vesicle has an excess area. The latter can be characterized by a dimensionless factor Δ, which is traditionally introduced via the relations

$$\mathcal{A} = (4\pi + \Delta) r_0^2, \qquad \mathcal{V} = 4\pi r_0^3/3, \tag{1}$$

where r_0 is a vesicle 'radius' determined by its volume. The excess area is a non-negative quantity: $\Delta \geqslant 0$, and its minimal value $\Delta = 0$ corresponds to the ideal spherical geometry. Nearly spherical (quasi-spherical) vesicles are characterized by the condition $\Delta \ll 1$.

The energy of the membrane is determined by its bending distortions and can be written as the following surface integral [36]–[39]:

$$\mathcal{F}^{(\mathrm{b})} = \int \mathrm{d}A (\kappa H^2/2 + \bar{\kappa} K), \tag{2}$$

taken over the membrane position. Here κ and $\bar{\kappa}$ are bending modules, H and K are mean and Gaussian curvatures, respectively. They are related to the local curvature radii of the membrane, R_1 and R_2, as

$$H = R_1^{-1} + R_2^{-1}, \qquad K = R_1^{-1} R_2^{-1}. \tag{3}$$

In accordance with the Gauss–Bonnet theorem, the second term in the right-hand side of equation (2) is invariant under smooth deformations of the membrane shape. Therefore it is irrelevant for problems with fixed vesicle topology.

Note that we have also ignored the so-called spontaneous curvature term in the bending energy. In other words, the expression (2) implies that the membrane is symmetric, which is typical for lipid bilayers. Speaking more rigorously, we assume that the spontaneous curvature radius is much larger than the vesicle size. The assumption seems to be valid in most of the experiments with giant vesicles.

Besides the bending energy (2), the membrane is characterized by its surface tension σ. In our setup, surface tension is an auxiliary variable which ensures the membrane incompressibility by adjusting to the non-stationary vesicle shape. The value of the surface tension can vary significantly along the membrane.

2.2. Flow near the vesicle

We consider the case where both liquids, contained inside the vesicle and surrounding it, are Newtonian. Furthermore, we assume that the Reynolds number associated with the vesicle dynamics is vanishingly small, which is the case in microfluidics experiments, see [1]–[7]. Under these assumptions, the liquids can be described by the Stokes equation

$$\varrho\, \partial_t \boldsymbol{v} = \eta \nabla^2 \boldsymbol{v} - \nabla P, \tag{4}$$

where P is the pressure, $\boldsymbol{v}$ is the fluid velocity, ϱ is the mass density and η is its shear dynamic viscosity. Equation (4) has to be supplemented with the incompressibility condition $\nabla \boldsymbol{v} = 0$, which leads to the Laplace equation for the pressure, $\nabla^2 P = 0$.

We split up the flow near the vesicle into two parts: an external flow, which would be observed in the fluid in the absence of the vesicle, and an induced flow, which is excited as a

result of the vesicle reaction to the external flow. The external flow is assumed to be stationary, or slowly varying in time. One should remember that the vesicle is advected by the flow, and therefore the above assumption should be valid in the Lagrangian reference frame attached to the vesicle. Below, we neglect the term with the time derivative in equation (4) since the characteristic timescale associated with the vesicle dynamics is assumed to be large compared with the viscous relaxation time $\varrho r_0^2/\eta$.

We assume that the characteristic spatial scale of the external flow is much larger than the vesicle size. In this case the external velocity, $\boldsymbol{V}$, near the vesicle can be approximated by a linear profile, determined by a derivative matrix $\partial_k V_i$. The incompressibility condition implies that the matrix $\partial_k V_i$ is traceless. Generally, the external flow has two contributions, elongational and rotational:

$$\partial_k V_i = s_{ik} - \epsilon_{ikj}\omega_j, \tag{5}$$

where $\hat{s}$ is the strain matrix (symmetric part of the matrix $\partial_k V_i$), ϵ_{ikj} is an absolutely antisymmetric tensor and $\boldsymbol{\omega}$ is the angular velocity vector. The strain power can be characterized by its strength s, defined as $s^2 = (1/2)\mathrm{tr}\,\hat{s}^2$. Note that for a shear flow, $s = |\boldsymbol{\omega}| = \dot{\gamma}/2$, where $\dot{\gamma}$ is the shear rate.

The fluids inside and outside the vesicle are generally different. The external fluid viscosity is designated by η and the viscosity of the internal fluid is designated by $\tilde{\eta}$. An important parameter that controls the tank-treading to tumbling transition is the viscosity contrast $\tilde{\eta}/\eta$. The limit where the viscosity contrast tends to infinity corresponds to a solid body behavior of the vesicle, which preserves its equilibrium shape. The solid body behavior in the external flow was first analyzed by Jeffery [40], who studied ellipsoidal particles in planar flows.

The membrane is advected by the fluid: the velocity field $\boldsymbol{v}$ is continuous on the membrane and determines the membrane velocity as well as the fluid velocity. For the relatively slow processes that we are investigating, the membrane can be treated as locally incompressible, which leads to the condition

$$\partial_i^{\perp} v_i = 0, \qquad \text{where } \partial_i^{\perp} = \delta_{ik}^{\perp}\partial_k, \tag{6}$$

being satisfied on the membrane. Here $\delta_{ik}^{\perp}$ is the projector to the membrane; it can be written as $\delta_{ik}^{\perp} = \delta_{ik} - l_i l_k$, where $\boldsymbol{l}$ is the unit vector normal to the membrane. The $3d$ incompressibility condition $\boldsymbol{\nabla v} = 0$ together with equation (6) leads to the relation $l_i l_k \partial_i v_k = 0$, valid at both sides of the membrane.

2.3. Membrane stress

The membrane reaction is characterized by its surface stress tensor $T_{ik}^{(\mathrm{s})}$. There are three contributions to the tensor related to the bending energy (2), to the surface tension of the membrane and to the internal membrane viscosity:

$$T_{ik}^{(\mathrm{s})} = T_{ik}^{(\kappa)} - \sigma\delta_{ik}^{\perp} - \zeta\delta_{ij}^{\perp}\delta_{kn}^{\perp}(\partial_j v_n + \partial_n v_j). \tag{7}$$

Here σ is the surface tension coefficient and ζ is the membrane ($2d$) viscosity. Note that the surface tension σ plays an auxiliary role being adjusted to other stresses ensuring the local membrane incompressibility. An expression for the bending contribution to the surface stress tensor was found in the work [41] (see also the book [42]). It can be written as

$$T_{ik}^{(\kappa)} = \kappa\left(-\tfrac{1}{2}H^2\delta_{ik}^{\perp} + H\partial_i^{\perp} l_k - l_i\partial_k^{\perp} H\right), \tag{8}$$

where $H = \nabla\boldsymbol{l}$ is the membrane mean curvature and $\partial_i^{\perp}$ is defined by equation (6).

The surface force $\boldsymbol{f}$ (force per unit area) associated with the membrane stress tensor $T_{ik}^{(s)}$ can be calculated as $f_i = -\partial_k^{\perp} T_{ik}^{(s)}$. There are three contributions to the surface force, which can be found from the expressions (7) and (8):

$$\boldsymbol{f} = \boldsymbol{f}^{(\kappa)} + \boldsymbol{f}^{(\sigma)} + \boldsymbol{f}^{(v)}, \tag{9}$$

where

$$f_i^{(\kappa)} = \kappa \left[H \left(H^2/2 - 2K \right) + \Delta^{\perp} H \right] l_i, \tag{10}$$

$$f_i^{(\sigma)} = -H\sigma l_i + \partial_i^{\perp}\sigma, \tag{11}$$

$$f_i^{(v)} = \zeta \left[\delta_{ij}^{\perp} \Delta^{\perp} v_j - H l_n \partial_i^{\perp} v_n - 2 l_i (\partial_n^{\perp} l_j) \partial_j^{\perp} v_n \right]. \tag{12}$$

Here, again, H and K are the mean curvature and the Gaussian curvature of the membrane, and $\Delta^{\perp}$ is the Laplace–Beltrami operator, $\Delta^{\perp} = \partial_i^{\perp}\partial_i^{\perp}$, associated with the membrane. Note that the expression for the force (10) can also be derived by calculating the variation of the bending energy (2) due to infinitesimal membrane deformations [43].

The surface force $\boldsymbol{f}$ is compensated by the momentum flux from the surrounding medium to the membrane. This flux consists of two parts, related to the fluid pressure and to the fluid viscosity. As a result of the balance, we find the following relations:

$$-\kappa[H(H^2/2 - 2K) + \Delta^{\perp} H] + \sigma H + 2\zeta \partial_i^{\perp} l_n \partial_n^{\perp} v_i = P_{\text{in}} - P_{\text{out}}, \tag{13}$$

$$\partial_i^{\perp}\sigma + \zeta(\delta_{ij}^{\perp}\Delta^{\perp} v_j - H l_n \partial_i^{\perp} v_n) = l_k \left[\tilde{\eta} (\partial_i v_k + \partial_k v_i)_{\text{in}} - \eta (\partial_i v_k + \partial_k v_i)_{\text{out}} \right], \tag{14}$$

for the normal and tangential to the membrane components of the force. Here, we assumed that the unit vector $\boldsymbol{l}$ is directed outside the vesicle and the subscripts 'in' and 'out' label regions inside and outside the vesicle, respectively. Thus, $P_{\text{in}} - P_{\text{out}}$ is the pressure difference between the inner and outer regions that is the pressure jump on the membrane. Note that a fluid viscous contribution is absent in equation (13) due to the condition $l_i l_j \partial_i v_j = 0$, following from the membrane incompressibility (see above).

To find the velocity field at a given membrane shape one should solve the stationary Stokes equation $\eta \nabla^2 \boldsymbol{v} = \nabla P$ (inside and outside the vesicle) with the boundary conditions (6), (13) and (14) to be satisfied on the membrane. An additional boundary condition reads that $\boldsymbol{v} \to \boldsymbol{V}$ far away from the membrane. Note that due to linearity of the equations and the boundary conditions for the velocity, a solution of the equations can be written as a sum

$$\boldsymbol{v} = \boldsymbol{v}^{(s)} + \boldsymbol{v}^{(\omega)} + \boldsymbol{v}^{(\kappa)}, \tag{15}$$

where $\boldsymbol{v}^{(s)}$ and $\boldsymbol{v}^{(\omega)}$ are proportional to the strain and to the angular velocity related to the gradient of the external flow (5), and $\boldsymbol{v}^{(\kappa)}$ is proportional to the bending modulus κ. Of course, all terms in the right-hand side of equation (15) are complicated functions of the vesicle shape.

Note that without the terms with the factor κ the boundary conditions (13) and (14) are invariant under the transformation $\boldsymbol{v} \to -\boldsymbol{v}$, $P \to -P$ and $\sigma \to -\sigma$. The stationary Stokes equation $\eta \nabla^2 \boldsymbol{v} = \nabla P$ and the boundary condition (6) are also invariant under the transformation. The kinematic relation (19) becomes invariant under the transformation if one adds the rule $t \to -t$. Therefore, in this approximation, the backward in time evolution of the displacement u is equivalent to the direct evolution in the external flow with the velocity $-\boldsymbol{V}$. Since the vesicle dynamics is determined by the matrix (5), the transformation $\boldsymbol{V} \to -\boldsymbol{V}$ is equivalent to space inversion. That produces some additional symmetry leading to important consequences for the vesicle dynamics. We examine the consequences in more detail for planar external velocity fields.

2.4. Membrane shape parametrization

In the following, we use a particular parametrization of the vesicle shape

$$r = r_0[1 + u(\theta, \varphi)], \tag{16}$$

where r_0 is determined by the relation (1). Here r, θ and φ are the radius, azimuthal angle and polar angle in the reference frame with the origin in the center of the vesicle. The dimensionless radial displacement u characterizes deviations of the membrane shape from the spherical one.

There are two constraints imposed on the function $u(\theta, \varphi)$ due to the volume and surface area conservation conditions (1). In terms of the displacement u, the conditions can be rewritten as

$$\int \mathrm{d}\varphi\, \mathrm{d}\theta\ \sin\theta\, (u + u^2 + u^3/3) = 0, \tag{17}$$

$$\Delta = \int \mathrm{d}\varphi\, \mathrm{d}\theta\ \sin\theta \left\{ (1+u) \left[(1+u)^2 + (\partial u/\partial\theta)^2 + \frac{(\partial u/\partial\varphi)^2}{\sin^2\theta} \right]^{1/2} - 1 \right\}. \tag{18}$$

The relations (17) and (18) are formally exact. However, they can be directly used only if $u(\theta, \varphi)$ is a single-valued function.

Advection of the membrane by the surrounding fluid implies the following kinematic relation:

$$\partial_t u = \frac{1}{r_0} v_r - \frac{1}{r} \left(v_\theta \partial_\theta u + \frac{1}{\sin\theta} v_\varphi \partial_\varphi u \right). \tag{19}$$

Here v_r, v_θ and v_φ are spherical components of the velocity v taken at the membrane, that is, at r determined by equation (16). Again, the relation (19) is formally exact, but can be directly used only if $u(\theta, \varphi)$ is a single-valued function.

3. Weak flows

The vesicle shape depends on the strength of the external flow. In weak flows it is close to an equilibrium one, whereas in strong flows it is determined by the velocity gradient matrix (5). In this section, we consider the first case. We discuss the equilibrium vesicle shape that can be found by minimizing the vesicle-free energy [44]. For nearly spherical vesicles it is a prolate ellipsoid. Then we develop a phenomenology for the vesicle dynamics in weak flows where the vesicle shape can be completely described by the main axis orientation.

3.1. Perturbation expansion

Below, we consider nearly spherical (quasi-spherical) vesicles for which the excess area parameter Δ introduced by equation (1) is small, $\Delta \ll 1$. In this case the dimensionless displacement u is small as well and it is possible to develop a perturbation theory that is constructed as an expansion over u. This perturbation series is a basis for subsequent consideration.

It is natural to represent the function $u(\theta, \varphi)$ as a sum over spherical harmonics:

$$u = \sum_{l,m} u_{l,m} \mathcal{Y}_{l,m}(\theta, \varphi), \tag{20}$$

where $\mathcal{Y}_{l,m}$ are spherical functions. The homogeneous contribution to u, that is, $u_{0,0}$, can be expressed via the inhomogeneous one (related to harmonics with $l > 0$) from the relation (17), which reflects the volume conservation. Substituting the resulting expression for the zero angular harmonic into equation (18), we obtain an expression for Δ whose expansion over u starts from the second-order term. Therefore, the displacement u can be estimated as $\sqrt{\Delta}$.

The contributions to u related to different angular harmonics play different roles. The zero angular harmonic can be excluded from the beginning, as we have explained. The first-order angular harmonic corresponds to a shift of the vesicle as a whole, and is not important in our analysis. The most essential role is played by the second angular harmonic which determines the vesicle shape. The relaxation rates of higher-order spherical harmonics are much larger in comparison with the second one. Therefore, for the relatively slow processes that we are considering, higher-order harmonics are weakly excited and their contribution to the vesicle shape can be neglected.

To avoid a misunderstanding, let us stress that the last assertion is valid only for quasi-stationary external flows. As was discovered experimentally, see [45], and explained theoretically, see [46], under some conditions (abrupt inversion of the external purely elongational flow) high-order angular harmonics can be generated, leading to the phenomenon called vesicle wrinkling [45].

3.2. Equilibrium

In the absence of an external flow, the vesicle has an equilibrium shape that can be found by minimization of the effective free energy

$$\mathcal{F} = \mathcal{F}^{(\mathrm{b})}(u) + \bar{\sigma}\, r_0^2 \Delta(u), \tag{21}$$

where the first term is determined by the expression (2) and $r_0^2\Delta$ is the membrane excess area expressed in terms of the displacement u. The Lagrange multiplier $\bar{\sigma}$, related to a fixed value of the membrane area, coincides with the equilibrium value of the surface tension. The second Lagrange multiplier (related to the volume $\mathcal{V}$) is absent in equation (21) since we imply that the zero angular harmonic in an expansion of the displacement u is expressed via other ones from the relation (17). Therefore, the volume conservation is automatically satisfied in our scheme.

If Δ is small, the principal contributions to the energy (2) as well as to the excess area are of the second order in u. It is convenient to write the contributions in terms of the coefficients $u_{l,m}$ of the expansion (20) of $u(\theta, \varphi)$ over the angular harmonics:

$$\mathcal{F}^{(2)} = \frac{\kappa}{2} \sum_{l \geqslant 2, m} (l+2)(l+1)l(l-1) \left|u_{l,m}\right|^2 + \frac{1}{2}\bar{\sigma} r_0^2 \sum_{l \geqslant 2, m} (l+2)(l-1) \left|u_{l,m}\right|^2. \tag{22}$$

Note that the first angular harmonic (with $l = 1$) is absent in the expansions. The reason is that it corresponds to a vesicle shift as a whole, which does not change the energy and the area of the vesicle. As follows from equation (22), the minimum of free energy is achieved if only the second-order harmonic is excited. In this case the equilibrium value of the surface tension is $\bar{\sigma} = -6\kappa/r_0^2$.

Note that the expansion (22) is degenerated in m. Therefore, in order to determine the vesicle equilibrium shape, that is, $u_{2,m}$, one should take into account terms of higher order in the expansion of the effective free energy (21), which violate the degeneracy. In the main approximation, it is enough to keep the third-order term in the expansion.

For a subsequent analysis, it is convenient for us to use the following real valued basis:

$$\psi_1 = \frac{\sqrt{5}}{4\sqrt{\pi}}(1-3\cos^2\theta), \qquad \psi_2 = \frac{\sqrt{15}}{2\sqrt{\pi}}\sin(2\theta)\cos\varphi,$$

$$\psi_3 = \frac{\sqrt{15}}{2\sqrt{\pi}}\sin(2\theta)\sin\varphi, \qquad \psi_4 = \frac{\sqrt{15}}{4\sqrt{\pi}}\sin^2\theta\cos(2\varphi),$$

$$\psi_5 = \frac{\sqrt{15}}{4\sqrt{\pi}}\sin^2\theta\sin(2\varphi), \tag{23}$$

instead of the traditional angular functions $\mathcal{Y}_{2,m}$. The functions ψ_μ satisfy the following normalization condition:

$$\int \mathrm{d}\varphi\,\mathrm{d}\theta\ \sin\theta\,\psi_\mu\psi_\nu = \delta_{\mu\nu}. \tag{24}$$

The second-order harmonic contribution to u can be rewritten as follows:

$$u(\theta,\varphi) = \sum_{\nu=1}^{5} u_\nu\,\psi_\nu(\theta,\varphi), \tag{25}$$

where u_ν are some real coefficients.

Expanding the bending energy (2) and the excess area Δ up to the third order in u, one obtains

$$\mathcal{F}^{(3)} = 12\kappa\left(u_\mu u_\mu - \Xi_{\mu\nu\lambda}u_\mu u_\nu u_\lambda\right) + \bar{\sigma}r_0^2\Delta^{(3)}, \tag{26}$$

$$\Delta^{(3)} = 2u_\mu u_\mu - 2\Xi_{\mu\nu\lambda}u_\mu u_\nu u_\lambda/3, \tag{27}$$

in terms of the coefficients of the expansion (25). Here summation over repeated indices is implied and we introduced the following object:

$$\Xi_{\mu\nu\lambda} = \int \mathrm{d}\varphi\,\mathrm{d}\theta\ \sin\theta\,\psi_\mu\psi_\nu\psi_\lambda. \tag{28}$$

All the components of the object are of the order of unity, and can be found from the definition (28) and the expressions (23).

After minimizing the free energy (26) over u_μ and calculating the Lagrangian multiplier $\bar{\sigma}$ from the condition $\Delta = \Delta^{(3)}$, one obtains

$$1 + \frac{\bar{\sigma}r_0^2}{6\kappa} = \frac{\sqrt{15}}{14\sqrt{\pi}}\sqrt{\Delta}. \tag{29}$$

This is the correction related to the third-order term in the expansion of the free energy. The minimum of the energy corresponds to a prolate uniaxial ellipsoid. If the principal axis of the ellipsoid is directed along the Z-axis its shape is determined by the relation $u_1 = -\sqrt{\Delta/2}$, that is,

$$u = \frac{\sqrt{5\Delta}}{4\sqrt{2\pi}}(3\cos^2\theta - 1). \tag{30}$$

Substituting the expression (29) into the effective free energy (26) we find that the coefficient in front of $u_\mu u_\mu$ in the expression is estimated as $\kappa\sqrt{\Delta}$. It contains an extra small factor $\sqrt{\Delta}$ in comparison with the natural estimation κ. Thus, both, second-order and third-order, terms in the free energy (26) are of the same order. That gives a formal justification to the procedure outlined in this subsection.

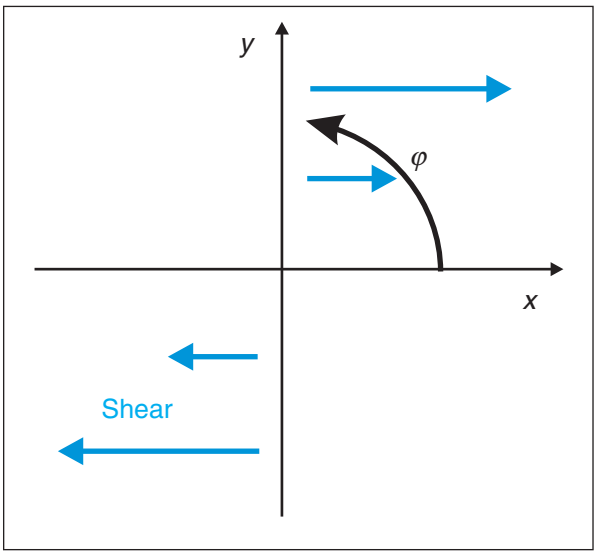

Figure 2. Reference frame related to shear flow.

3.3. Weak external flow, phenomenology

Here, we analyze the case of weak external flows that cannot significantly distort the vesicle equilibrium shape. As we established in the preceding subsection, the equilibrium shape of a nearly spherical vesicle is the prolate ellipsoid possessing uniaxial symmetry. The orientation of such an ellipsoid in space can be characterized by a unit vector $\boldsymbol{n}$ directed along the principal axis of the ellipsoid. If the principal axis is parallel to the Z-axis the vesicle shape is determined by the expression (30). Note that the vectors $\boldsymbol{n}$ and $-\boldsymbol{n}$ describe the same physical state since the ellipsoid is invariant under inversion.

One can formulate a phenomenological equation for the dynamics of $\boldsymbol{n}$ in a weak external flow: $\partial_t n_i = D_{ijk}\partial_k V_j$, where $\partial_k V_j$ is the velocity gradient matrix of the external flow and D_{ijk} is some tensor related to the vesicle orientation. Due to the symmetry $\boldsymbol{n} \to -\boldsymbol{n}$ the tensor D_{ijk} contains only odd powers of $\boldsymbol{n}$. Using the relation $\boldsymbol{n}^2 = 1$, that is, $n_i D_{ijk} = 0$, we arrive at the following general form:

$$\partial_t n_i = \left[(n_k\delta_{ij} - n_j\delta_{ik})/2 + D\left(n_k\delta_{ij}/2 + n_j\delta_{ik}/2 - n_i n_j n_k\right)\right]\partial_k V_j, \tag{31}$$

containing a single dimensionless parameter D. In order to derive this equation, we exploited the fact that the vesicle dynamics should be purely rotational, $\partial_t n_i = \epsilon_{ijk}\omega_j n_k$, in the case of an external flow $\partial_j V_i = -\epsilon_{ijk}\omega_k$ corresponding to a solid rotation. The factor D in equation (31) depends on relative viscosities of the membrane and internal/external fluids and on the excess area parameter Δ. An explicit expression for D will be derived *ab initio* in section 7.

For an external shear flow, it is convenient to use the following parametrization of the unit vector $\boldsymbol{n}$:

$$\boldsymbol{n} = (\cos\vartheta\cos\phi, \cos\vartheta\sin\phi, \sin\vartheta)\,. \tag{32}$$

The components here are written in the Cartesian reference frame attached to the flow: the X-axis is directed along the velocity and the Z-axis is antiparallel to the angular velocity vector $\boldsymbol{\omega}$ (see figure 2 for clarification). Substituting the expression (32) and the shear velocity gradient

matrix with a single nonzero component $\partial_y V_x = \dot{\gamma}$ into equation (31), one obtains

$$\dot{\gamma}^{-1}\partial_t \phi = (D/2)\cos(2\phi) - 1/2, \tag{33}$$

$$\dot{\gamma}^{-1}\partial_t \vartheta = -(D/4)\sin(2\vartheta)\sin(2\phi). \tag{34}$$

Note that the dynamic equation for the angle ϕ is separated. The equations (33) and (34) resemble the equations for a single polymer dynamics examined in [47].

The solutions of (33) and (34) correspond to either tank-treading or tumbling types of vesicle motion. For $|D| > 1$, the tank-treading regime is realized, with a steady tilt angle (between the vector $\boldsymbol{n}$ and the velocity direction)

$$\phi_* = (1/2)\arccos(1/D). \tag{35}$$

Otherwise, for $|D| < 1$, the tumbling regime takes place: the vector $\boldsymbol{n}$ experiences a time-periodic motion with an average rotation in the shear plane. Thus, the value $D = 1$ corresponds to the tank-treading to tumbling transition. As follows from equation (33), the transition is described by the saddle–node bifurcation.

4. General dynamic equation

In this section, we derive a dynamic equation for the dimensionless displacement u. The derivation procedure consists of two steps. First, one finds the velocity profile for a given vesicle shape that is for a given displacement field $u(\theta, \varphi)$. Next, one uses the kinematic relation (19), which leads to a closed equation for the field u. Of course, the expression for $\partial_t u$ is a nonlinear function of u. We find the principal terms of its expansion in u.

4.1. Closed equation

In order to apply the procedure described above, we employ the generalization of the Lamb scheme. In accordance with Lamb [48] (see also [49]), a solution of the stationary Stokes equation can be explicitly expressed via the velocity field taken at a sphere both for the internal and for the external problems. The Lamb scheme gives the exact solutions of the Stokes equation. The scheme can be directly applied to a spherical solid body immersed in a fluid or to a spherical cavity filled up with a fluid. Then the value of the velocity field at an arbitrary point is expressed in terms of its surface value. For a nearly spherical vesicle the scheme is slightly modified. Namely, one should express the velocity field via its value on the sphere of radius r_0. These values can be obtained by analytical continuation of the internal and external velocity fields and are slightly different in the cases. Then the boundary values are represented as an expansion over the displacement u. Thus, the formally exact Lamb scheme becomes approximate when one truncates the expansion. In our case, $\sqrt{\Delta}$ is the small parameter, which controls the error associated with the series truncation. We therefore expect our results to be asymptotically exact in the limit $\Delta \to 0$, which corresponds to spherical vesicles.

In the zeroth approximation, one can ascribe the membrane velocity directly to the sphere $r = r_0$ ignoring deviations of the vesicle shape from the sphere. Keeping then the lowest in u terms in all expressions, one obtains an equation for the displacement u equivalent to the one discussed in [8, 25]. However, as we demonstrated in [26], such an approximation is not self-consistent because it leads to dynamics sensitive to initial conditions. One can overcome this sensitivity only by accounting for high-order terms in u.

Here, we derive an equation for the displacement u in the approximation where the membrane velocity and the boundary conditions (13) and (14) are related to the sphere $r = r_0$. Corrections to the equations associated with the deviations of the vesicle shape from the sphere are small in u. However, for the reasons formulated above, we keep the leading nonlinear in u term in the expression for the boundary force (9). Further, we justify the approximation.

Note, first of all, that the variational derivative of the effective free energy (21) can be represented as

$$\frac{\delta \mathcal{F}}{\delta u} \equiv r_0 \left\{ -\kappa [H(H^2/2 - 2K) + \Delta^{\perp} H] + \bar{\sigma} H \right\}.$$

Therefore the boundary condition (13) can be rewritten as

$$\delta \mathcal{F}/\delta u = -2\tilde{\sigma} + r_0 P_{\text{in}} - r_0 P_{\text{out}}. \tag{36}$$

Here, we divided the surface tension, σ, into a homogeneous, $\bar{\sigma}$, and an inhomogeneous, $\tilde{\sigma}$, parts. By definition, the zero angular harmonic is absent in $\tilde{\sigma}$. Next, for the sphere $r = r_0$ the average curvature is $H = 2/r_0$ and $\partial_i^{\perp} l_n \partial_n^{\perp} v_i \propto \delta_{in}^{\perp} \partial_n^{\perp} v_i = 0$, which explains the validity of the expression (36).

To find the inhomogeneous part of the surface tension, $\tilde{\sigma}$, one has to use the second boundary condition, (14). Taking the derivative $\partial_i^{\perp}$ of the condition (14) and relating the result to the sphere $r = r_0$, one obtains

$$\begin{aligned} l(l+1)\sigma_l - 2\zeta(l+2)(l-1)v_{r,l} = \tilde{\eta}\left[(l+2)(l-1)v_{r,l} + r_0^2 \partial_r^2 v_{r,l}\right]_{\text{in}} \\ -\eta\left[(l+2)(l-1)v_{r,l} + r_0^2 \partial_r^2 v_{r,l}\right]_{\text{out}}, \end{aligned} \tag{37}$$

where σ_l and $v_{r,l}$ are contributions to the surface tension and to the radial velocity associated with the lth order angular harmonic. As above, the subscripts 'in' and 'out' are related to the interior and exterior regions of the vesicle.

Applying the Lamb scheme to the sphere $r = r_0$, one finds for the internal problem

$$P_{\text{in}} = -\tilde{\eta} \sum_l \frac{r^l}{r_0^l} \frac{(l-1)(2l+3)}{l} \partial_t u_l, \tag{38}$$

$$v_r = \sum_l \left(\frac{r^{l-1}}{r_0^{l-2}} \frac{l+1}{2} - \frac{r^{l+1}}{r_0^l} \frac{l-1}{2} \right) \partial_t u_l. \tag{39}$$

Here, we used the condition $\partial_r v_r(r_0) = 0$, following from the relation $l_i l_k \partial_i v_k = 0$ where $l_i = (\sin\theta\cos\varphi, \sin\theta\sin\varphi, \cos\theta)$ is the unit vector perpendicular to the sphere $r = r_0$. We substituted also $v_r(r_0) = r_0 \partial_t u$, which is the kinematic relation (19) taken in the main approximation in u.

For the external problem, one should separately analyze the external contribution $\boldsymbol{V}$ to the velocity since it does not tend to zero as $r \to \infty$. Substituting $\boldsymbol{v} = \boldsymbol{V} + \boldsymbol{w}$, one obtains

$$P_{\text{out}} = \eta \sum_l \frac{r_0^{l+1}}{r^{l+1}} \frac{(l+2)(2l-1)}{l+1} \partial_t u_l, \tag{40}$$

$$w_r = \sum_l \left(\frac{r_0^{l+1}}{r^l} \frac{l+2}{2} - \frac{r_0^{l+3}}{r^{l+2}} \frac{l}{2} \right) \partial_t u_l, \tag{41}$$

analogous to equations (38) and (39). Here, again, we used the incompressibility condition $\partial_r w_r(r_0) = 0$ and the kinematic relation $w_r = r_0 \partial_t u$. The expressions (40) and (41) should be modified for $l = 2$ because of the external flow. The modified incompressibility condition has the form $\partial_r w_{r,2}(r_0) + s_{ik} l_i l_k = 0$ and the modified kinematic condition is $\partial_t u_2 = w_{r,2} + r_0 s_{ik} l_i l_k$. This yields

$$P_{\mathrm{out},2} = \eta(4\partial_t u_{(2)} - 5 s_{ik} l_i l_k) r_0^3 / r^3, \tag{42}$$

$$w_{r,2} = \left(2\partial_t u_{(2)} - 5 s_{ik} l_i l_k / 2\right) r_0^3 / r^2 - \left(\partial_t u_{(2)} - 3 s_{ik} l_i l_k / 2\right) r_0^5 / r^4. \tag{43}$$

After collecting together the relations (36)–(43), we obtain a closed equation for the displacement u

$$\hat{a}(\partial_t - \omega \partial_\varphi) u = 10 s_{ij} l_i l_j - \frac{1}{\eta r_0} \frac{\delta \mathcal{F}}{\delta u}, \tag{44}$$

where $\hat{a}$ is a dimensionless operator with angular components

$$a_l = \frac{2l^3 + 3l^2 + 4}{l(l+1)} + \frac{2l^3 + 3l^2 - 5}{l(l+1)} \frac{\tilde{\eta}}{\eta} + \frac{l^2 + l - 2}{l(l+1)} \frac{4\zeta}{\eta r_0}.$$

We included in equation (44) a dependence on the rotational part of the external flow, which can be established by a discription of the nonlinear term in the kinematic relation (19).

Recall that the quantity $\bar{\sigma}$ entering the dynamic equation (44) through equation (21) is the surface tension σ averaged over angles. As previously, $\bar{\sigma}$ is an auxiliary quantity ensuring the surface conservation law. Let us stress that $\bar{\sigma}$ depends on time, adjusting to the current vesicle shape. Note that the strain and the rotation parts of the external flow are separated: the angular velocity $\boldsymbol{\omega}$ extends the time derivative (its effect is equivalent to passing to the rotating reference frame), whereas the strain matrix enters the term $s_{ij} l_i l_j$ playing a role similar to the free energy derivative. The reason is that the elongational part of the flow leads to some viscous dissipation, whereas solid rotation does not imply any dissipation.

4.2. Second-order angular harmonic

Equation (44) can be further simplified. First of all, one can keep the second- and third-order terms in the effective free energy (21). Higher-order terms in $\mathcal{F}$ are negligible since $u \ll 1$. The reason why one should keep the third-order term behind the dominant second-order ones is explained below. Next, the expansion of the term $s_{ij} l_i l_j$ does not contain any angular harmonics with $l > 2$, so this term does not push u outside the $l = 2$ subspace. Higher-order angular harmonics in u are excited by the high-order corrections to the free energy of the membrane and by the $s_{ij} l_i l_j$ term, which are both small compared with the terms corresponding to the second-order harmonics. The amplitude of high-order harmonics can be estimated as Δ, which should be compared with the $\sqrt{\Delta}$ amplitude of the second-order harmonic. Back-reaction of high-order harmonics on the second one can also be neglected as they produce an effective force which can be estimated as $\Delta^{3/2}$ and is thus smaller than those are kept in the expansions presented below. Therefore one can use a reduced equation where u contains only second-order angular harmonics. The operator $\hat{a}$ in this case is reduced to a constant

$$a = \frac{16}{3}\left(1 + \frac{23}{32}\frac{\tilde{\eta}}{\eta} + \frac{\zeta}{2\eta r_0}\right), \tag{45}$$

depending on the viscosities. The constant a can be called a generalized viscosity contrast. Note that the limit $a \to \infty$ (where the internal fluid viscosity or the membrane viscosity tends to infinity) should correspond to a solid body behavior of the vesicle.

One can substitute the expression (26) into equation (44) and then project the equation to the subspace $l = 2$. Then equation (44) is reduced to

$$a\left[\partial_t u_\mu - \omega(\partial_\varphi u)_\mu\right] = 10(s_{ij}l_i l_j)_\mu - \frac{24}{\eta r_0}\left[\left(\frac{\kappa}{r_0^2} + \frac{\bar\sigma}{6}\right)u_\mu - \left(\frac{3\kappa}{2r_0^2} + \frac{\bar\sigma}{12}\right)\Xi_{\mu\nu\lambda}u_\nu u_\lambda\right], \tag{46}$$

where the subscripts in $(\partial_\varphi u)_\mu$ and $(s_{ij}l_i l_j)_\mu$ designate projections of the functions to the basis (23) calculated in accordance with equation (24).

The factor $\bar\sigma$ in equation (46) should be extracted from the condition $2u_\mu u_\mu = \Delta$, which is the leading order expansion of the area conservation constraint. Substituting the resulting value of $\bar\sigma$, one obtains

$$a\left[\partial_t u_\mu - \omega(\partial_\varphi u)_\mu\right] = \left(\delta_{\mu\rho} - \frac{2u_\mu u_\rho}{\Delta}\right)\left[10(s_{ij}l_i l_j)_\rho + \frac{24\kappa}{\eta r_0^3}\,\Xi_{\rho\nu\lambda}u_\nu u_\lambda\right]. \tag{47}$$

In accordance with equation (15), the right-hand side of equation (47) is a sum of two terms, proportional to the strain s_{ij} and to the bending module κ, whereas the ω-proportional term is included in the left-hand side of the equation. Note that the term proportional to κ is of the second order (the first-order term is absent), which formally justifies keeping this high-order term in the expansion of the free energy.

Deriving equation (47), we neglected terms of order su, which arise as corrections to the term $s_{ij}l_i l_j$. They are much less compared with the term with κ provided $s \ll \kappa\sqrt{\Delta}/(\eta r_0^3)$, which is the formal applicability condition of the equation. However, below we demonstrate that equation (47) can be applied to stronger flows, with $s \gtrsim \kappa\sqrt{\Delta}/(\eta r_0^3)$, as well.

4.3. Rescaled equation

After some rescaling, equation (47) is rewritten as

$$\left(\tau\,\partial_t - \frac{S\Lambda}{2}\partial_\varphi\right)U_\mu = (\delta_{\mu\rho} - U_\mu U_\rho)(S_\rho + \tilde\Xi_{\rho\nu\lambda}U_\nu U_\lambda), \tag{48}$$

where $\tilde\Xi = (7\sqrt{\pi}/\sqrt{5})\,\Xi$ and

$$U_\mu = \sqrt{2}u_\mu/\sqrt{\Delta}, \quad U_1^2 + \cdots + U_5^2 = 1. \tag{49}$$

The parameters in equation (48) are defined as follows:

$$\tau = \frac{7\sqrt{\pi}}{12\sqrt{10}}\frac{a\eta r_0^3}{\kappa\sqrt{\Delta}}, \qquad S = \frac{14\pi}{3\sqrt{3}}\frac{s\eta r_0^3}{\kappa\Delta}, \qquad \Lambda = \frac{\sqrt{3}}{4\sqrt{10\pi}}\frac{\sqrt{\Delta}a\omega}{s}, \tag{50}$$

where, as previously, $s^2 = s_{ij}s_{ij}/2$. The 'vector' S_μ in equation (48) has an absolute value S, given by equation (50); its 'direction' is determined by the projections of the object $s_{ij}l_i l_j$ to the basis (23), that is, the 'direction' is determined by the structure of the strain matrix s_{ij}. Therefore the two parameters, S and Λ, together with the 'direction' of the 'vector' S_μ completely determine the character of the vesicle dynamics in the external flow.

The quantity τ is the characteristic timescale of the vesicle relaxation. In comparison with the combination $\eta r_0^3/\kappa$, related to the external fluid, the time τ contains an additional factor a, reflecting the contributions of the internal fluid viscosity and the membrane viscosity into the relaxation, and also the factor $\Delta^{-1/2}$. This extra factor reflects the additional slowness of the second-order angular harmonic relaxation related to the degeneracy of the second-order contribution to free energy. Due to the degeneracy the relaxation is determined by the third order term in the effective free energy, which contains a smallness $\Delta^{1/2}$ in comparison with the energy of higher angular harmonics. Therefore the adiabaticity condition, enabling one to use the stationary Stokes equation, should be written as $\tau \gg \varrho r_0^2/\eta$, that is, $a\eta^2 r_0 \gg \rho\kappa\sqrt{\Delta}$. The inequality is valid because the radius r_0 is large (in comparison with the molecular length) and Δ is small.

The parameter S characterizes the relative strength of the external flow. The expression (50) for S can be explained as follows. The external viscous surface force ηs should be balanced by the surface tension $\bar{\sigma}$ times a variation of the vesicle curvature, which is estimated as $\sqrt{\Delta}/r_0$. Therefore $\bar{\sigma} \sim \eta s r_0/\sqrt{\Delta}$. It has to be compared with the 'anisotropic' correction $\delta\sigma$ to the equilibrium surface tension, which can be estimated as $\kappa\sqrt{\Delta}/r_0^2$, see equation (29). And S is just a ratio of the surface tension values: $S \sim \bar{\sigma}/\delta\sigma$. Corrections of the order su neglected in the equations (47) and (48) are much smaller than the κ-proportional term provided $s \ll \kappa\sqrt{\Delta}/(\eta r_0^3)$; the condition can be rewritten as $S \ll 1/\sqrt{\Delta}$, in terms of S.

The parameter Λ determines the relative strength of the rotational part of the external flow. Note that $\omega\tau \sim S\Lambda$. The condition $\Lambda \sim 1$ determines the angular velocity whose effect is comparable with the effect of the strain; the condition reads $\omega \sim s/(a\sqrt{\Delta})$. This characteristic angular velocity does not coincide with the characteristic value of s, which stresses again the different roles of the rotational and of the elongational parts of the external flow in the vesicle dynamics.

For a concrete analysis, it is convenient to pass from the variables U_μ (49) to another set of variables, 'angles' Φ, Θ, Ψ and J, defined as

$$U_1 = \sin\Theta\cos J, \qquad U_2 = \sin\Theta\,\sin J\,\cos\Psi, \qquad U_3 = \sin\Theta\,\sin J\,\sin\Psi,$$
$$U_4 = \cos\Theta\cos(2\Phi), \qquad U_5 = \cos\Theta\sin(2\Phi), \tag{51}$$

where Θ varies from $-\pi/2$ to $\pi/2$, J varies from 0 to $\pi/2$, Ψ varies from $-\pi$ to π, and Φ varies from $-\pi/2$ to $\pi/2$. The representation (51) automatically satisfies the normalization condition (49) and contains, respectively, four independent parameters instead of five components U_μ. Note that the equilibrium vesicle shape characterized by the principal axis direction (32) is written as

$$\sin\Theta = -\sqrt{1-(3/4)\sin^4\vartheta}, \qquad \Phi = \Psi = -\phi, \qquad \tan J = \frac{2\sqrt{3}\sin(2\vartheta)}{1+3\cos(2\vartheta)}, \tag{52}$$

in terms of the 'angles'.

5. Planar external flow

We start to discuss the case of a planar external flow, where the fluid velocity vector $\boldsymbol{V}$ lies in a plane and is independent of a coordinate normal to the plane. One particular realization we have in mind is the shear flow where the elongational and the rotational contributions are in

balance. However, one can consider an arbitrary relation between the contributions, from purely elongational flows to solid rotation-type flows. All the cases are included in our scheme. In this section, we derive the general equation describing the vesicle dynamics in an external planar flow and give a preliminary analysis of types of its solution.

5.1. General consideration

For the planar velocity field, the only nonzero elements of the velocity gradient matrix $\partial_j V_i$ are related to the plane, so it is a 2×2 traceless matrix. We choose X- and Y-axes of our reference system parallel to the plane and assume (without any loss of generality) that the diagonal elements of the matrix $\partial_j V_i$ are zero. Two non-diagonal components of the matrix completely determine the planar flow; they can be parameterized in terms of the strain s and of the angular velocity ω as $\partial_y V_x = s + \omega$ and $\partial_x V_y = s - \omega$. In particular, for an external shear flow with the velocity directed along the X-axis the only nonzero element of the matrix is $\partial_y V_x = \dot{\gamma}$, then $\omega = s = \dot{\gamma}/2$. One can check that in the reference frame the only nonzero element of the 'vector' S_μ in equation (48) is $S_5 = S$. Thus the two parameters, S and Λ, completely determine the type of vesicle dynamics.

We will work in terms of the 'angles' Φ, Θ, Ψ and J, introduced by equation (51). They completely determine the vesicle shape if the second-order angular harmonic is leading. The vesicle displacement u defined by equation (16) is determined by the following expression:

$$u \propto \sin\Theta \cos J\, \psi_1 + \sin\Theta\, \sin J\, \cos\Psi\, \psi_2 + \sin\Theta\, \sin J\, \sin\Psi \psi_3 + \cos\Theta \cos(2\Phi)\psi_4 + \cos\Theta \sin(2\Phi)\psi_5, \tag{53}$$

where the functions ψ_i are defined by equation (23).

For the planar external flow and in terms of the 'angles', equation (48) is rewritten as

$$\tau \partial_t \begin{pmatrix} \Theta \\ \Phi \\ J \\ \Psi \end{pmatrix} = S \begin{pmatrix} g_\Theta \\ g_\Phi \\ 0 \\ 0 \end{pmatrix} - \frac{S\Lambda}{2} \begin{pmatrix} 0 \\ 1 \\ 0 \\ 1 \end{pmatrix} + \begin{pmatrix} f_\Theta \\ f_\Phi \\ f_J \\ f_\Psi \end{pmatrix}, \tag{54}$$

where

$$g_\Theta = -\sin(\Theta)\sin(2\Phi), \quad g_\Phi = (1/2)\cos(2\Phi)\sec\Theta, \tag{55}$$

$$\begin{aligned} f_\Theta &= \tfrac{1}{32}\{-4\cos J \cos\Theta \sin^2 J + [33\cos J - \cos(3J)]\cos(3\Theta) \\ &\quad - 4\sqrt{3}\cos[2(\Phi-\Psi)][\sin\Theta - 3\sin(3\Theta)]\sin^2 J\}, \\ f_\Phi &= -\tfrac{1}{4}\sqrt{3}\sin^2 J \sin\Theta \sin[2(\Phi-\Psi)]\tan\Theta, \\ f_J &= \tfrac{1}{8}\{-8\csc\Theta \sin J + [11\sin J - \sin(3J)]\sin\Theta \\ &\quad + 4\sqrt{3}\cos\Theta\cos[2(\Phi-\Psi)]\sin(2J)\}, \\ f_\Psi &= \sqrt{3}\,\cos\Theta\,\sin[2(\Phi-\Psi)]. \end{aligned} \tag{56}$$

Again, equation (54) is in accordance with the decomposition (15): the first term in the right-hand side of equation (54) is proportional to the elongational part of the external flow, the second term is proportional to its rotational part, and the last term is related to the membrane bending elasticity.

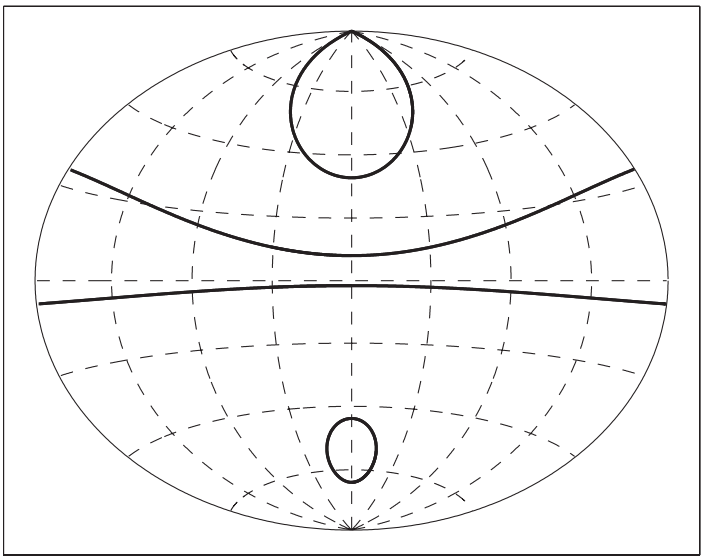

Figure 3. Vesicle dynamics on the Θ–Φ atlas.

5.2. Symmetric solution

It follows from equations (54) that there exists a solution with $J = 0$. This is a consequence of the geometry: the planar flow is invariant under reflection with respect to the flow plane. Due to this symmetry, there exists a θ-symmetric solution for the displacement u, corresponding to $J = 0$.

If $J = 0$, then the displacement u has the following angular dependence:

$$u \propto \cos\Theta \sin^2\theta \cos(2\varphi - 2\Phi) + \sin\Theta \frac{1 - 3\cos^2\theta}{\sqrt{3}}, \tag{57}$$

as follows from equations (23) and (53). Therefore the 'angle' Φ characterizes the vesicle orientation in the X–Y plane, whereas the 'angle' Θ determines the vesicle shape. The system of equations (54) is reduced at $J = 0$ to the following equations:

$$\tau \partial_t \Theta = -S \sin\Theta \sin(2\Phi) + \cos(3\Theta), \tag{58}$$

$$\tau \partial_t \Phi = \frac{S}{2}\left[\frac{\cos(2\Phi)}{\cos\Theta} - \Lambda\right]. \tag{59}$$

Note that the last, nonlinear in u, summand in equation (47) produces the only term, $\cos(3\Theta)$, in equation (58).

The tank-treading vesicle motion corresponds to a region of parameters S and Λ where the system of equations (58) and (59) has stable stationary points. The stationary points can be found by equating to zero the right-hand sides of the equations, which gives simple algebraic equations. The solutions of the equations are stable in a region where $\Lambda \lesssim 1$; its boundaries are established below.

For larger Λ the attractors of the system (58) and (59) are limit cycles. They correspond to either tumbling or trembling behavior. In the tumbling regime, the 'angle' Φ grows indefinitely, whereas in the trembling regime it oscillates in a restricted domain. To illustrate the assertion, it is convenient to represent the vesicle evolution on a geographic atlas, where Θ and Φ are the latitude and the longitude, correspondingly, see figure 3. The tank-treading regime corresponds

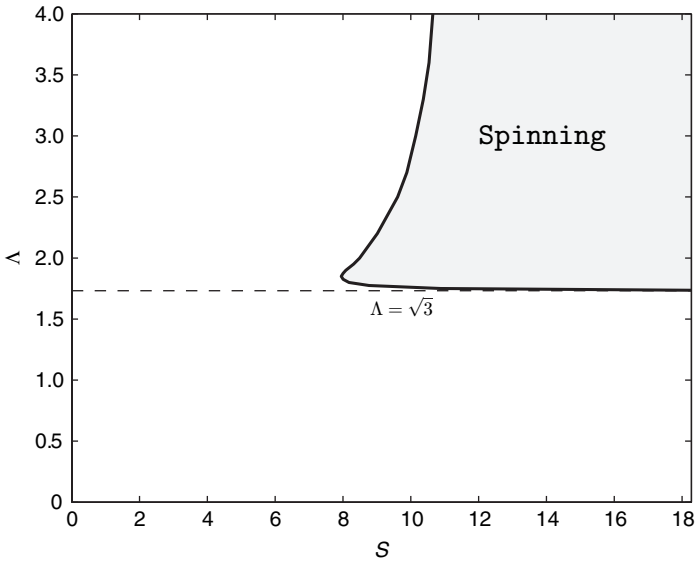

Figure 4. The region where spinning is realized.

to a fixed point on the atlas. The trembling regime corresponds to a closed curve, which does not surround a pole, whereas tumbling produces the curve containing the pole inside. In figure 3, such 'tumbling' curves terminate at the boundaries of the atlas having the same Θ on the boundaries, since points on the right and on the left boundaries of the atlas with the same latitudes are physically identical.

Let us stress that the trembling to tumbling transition does not imply any singularity (whereas the tank-treading to tumbling and the tank-treading to trembling transitions are realized through bifurcations, see the next section). It becomes clear if one imagines a gradual transformation of a cycle leading from trembling to tumbling. Obviously, the transformation is smooth even in the transition point from trembling to tumbling where the cycle crosses the pole.

5.3. Spinning

An investigation of the complete system of equations (54) indicates that at some values of the control parameters S and Λ, a novel regime of vesicle motion can be observed. The corresponding domain on the phase diagram is shown in figure 4. The vesicle shape in this regime is not symmetric under the reflection $z \to -z$ (or $\theta \to -\theta$). For $\Lambda \gg S$ the shape of the vesicle is close to the equilibrium one and the vesicle dynamics is reduced to the precession around the z-axis, with constant value of the angle between the z-axis and the principal axis of the vesicle. In contrast to the tumbling regime this angle is not equal to $\pi/2$. In the opposite limiting case $\Lambda \ll S$ the spinning motion is much more complicated. The principal axis is also not normal to z, but the precession is accompanied by periodic oscillations of the vesicle shape, in particular of its aspect ratio. Another way to imagine this regime is to think of $z \to -z$ asymmetric vesicle deformation spinning around the z-axis on top of a stationary $z \to -z$ symmetric ellipsoid with the main axis parallel to x.

As one can see from figure 4, spinning is observed at relatively large values of S and Λ. The vesicle shape in the spinning regime can be found analytically in the limiting cases of large Λ and large S; the corresponding analysis is presented in subsequent sections.

Note that spinning coexists with tumbling: these two types of motion are basins of attraction for different domains of the phase space of the dynamical system (54). Therefore a choice between spinning and tumbling depends on the initial vesicle shape. In real systems with non-vanishing thermal noise, one should observe a bistable vesicle behavior, where the tumbling oscillations are intermitted by the spinning ones. Our numerical experiments show that spinning and tumbling regimes have comparable basins of attraction for all S, Λ, so in real experiments both regimes should be observed with comparable probability. Near the boundary of the domain depicted in figure 4 the spinning regime loses its stability via a saddle–node bifurcation (passing to the tumbling regime).

6. Phase diagram of the system

It is convenient to construct a 'phase diagram' of the system in the S–Λ plane reflecting all types of vesicle motion. The structure of the phase diagram is determined by the transition lines between different regimes. There is a critical slowdown of the vesicle dynamics near tank-treading to tumbling and tank-treading to trembling transitions. That is why the vicinities of the transition lines need a special consideration. Note that there are no singularities in the vesicle dynamics near the trembling to tumbling transition. Indeed, from the point of view of the dynamics on the Φ–Θ atlas (see figure 3), there is no qualitative difference between cycles representing the tumbling and the trembling regimes and, consequently, the transition is smooth. Note also that there is a special point on the phase diagram where the tank-treading to tumbling and the tank-treading to trembling transition lines merge. An additional slowness of the vesicle dynamics near the special point occurs.

6.1. The tank-treading to trembling transition

As we have already noted, the tank-treading regime corresponds to the stationary points of the system (58) and (59). In order to study the stability of the stationary solutions we linearize the equations (58) and (59) near the stationary point:

$$\tau \partial_t \begin{pmatrix} \delta\Theta \\ \delta\Phi \end{pmatrix} = \hat{B} \begin{pmatrix} \delta\Theta \\ \delta\Phi \end{pmatrix}. \tag{60}$$

The stationary point is stable, if both the eigenvalues of the matrix $\hat{B}$ have negative real parts. Thus the stability conditions are $\mathrm{tr}\, B < 0$ and $\det B > 0$.

The tank-treading to trembling transition is determined by the condition $\mathrm{tr}\, \hat{B} = 0$ where $\hat{B}$ is the stability matrix introduced by equation (60) for the symmetric solution. Using the system (58) and (59) one can rewrite the condition $\mathrm{tr}\, \hat{B} = 0$ as a function $\Lambda = \Lambda_*(S)$ where

$$\Lambda_* = \sqrt{2}\sqrt{1 - 1/S^2}. \tag{61}$$

Here S varies from $\sqrt{3}$ to ∞, and Λ_* varies from $2/\sqrt{3}$ to $\sqrt{2}$. The transition curve, determined by equation (61), is plotted in red in figure 5. The curve starts from the special point $S = \sqrt{3}$, $\Lambda = 2/\sqrt{3}$ (the point e_1 in figure 5) and goes to the right.

For clarity, we kept only two phases corresponding to the tank-treading and trembling regimes on figure 5 where the vicinity of the special point e_1 is presented. Note that there is a region of parameters near the special point where two different tank-treading regimes coexist. In figure 5, we have shown only one of the tank-treading regimes, obtained by continuation from

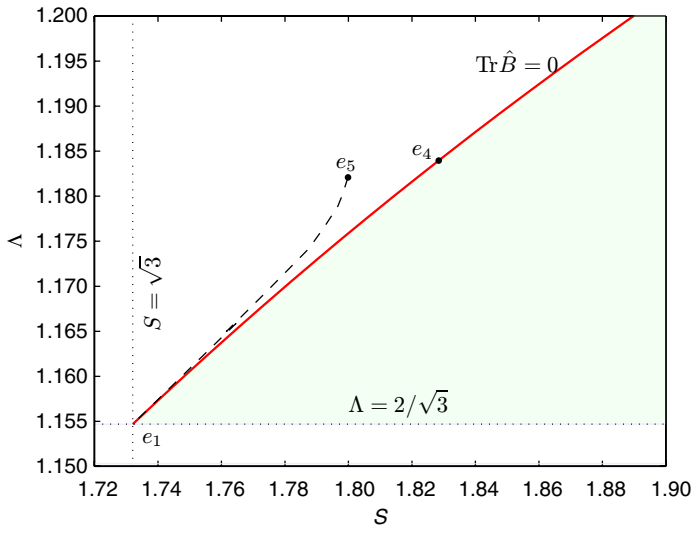

Figure 5. Phase diagram in the vicinity of the special point. Tank-treading to trembling transition.

the right region. The transition between the 'right' tank-treading and trembling occurs at the red curve. The dashed curve in figure 5 which was obtained numerically represents the stability boundary of the trembling regime. The curve terminates at the point e_5. Therefore, trembling motion is stable between the red and the dashed curves and above the point e_5. Left of the dashed curve the trembling regime becomes unstable, and it transforms into the tank-treading one.

Expanding equations (58) and (59) at a given S near the point (61), one derives the following equation:

$$\tau\,\partial_t Z = \varepsilon Z - \mathrm{i}\sqrt{S^2-3}\,Z - K|Z|^2 Z, \tag{62}$$

for a complex variable Z. Here

$$\varepsilon = \frac{8S\sqrt{S^2-1}}{S^2-3}(\Lambda-\Lambda_*), \qquad K = \frac{2\sqrt{2}\sqrt{S^2-1}(S^2+5)}{(S^2-3)^{3/2}},$$

and the variable Z is related to the deviation of the 'angles' from their stationary values as

$$\begin{pmatrix}\sqrt{2}\delta\Theta\\ \delta\Phi\end{pmatrix} = \begin{pmatrix}\mu^{-1}-\mathrm{i}\mu & \mu^{-1}+\mathrm{i}\mu\\ -\mu^{-1}-\mathrm{i}\mu & -\mu^{-1}+\mathrm{i}\mu\end{pmatrix}\begin{pmatrix}Z\\ Z^*\end{pmatrix},$$

where

$$\mu = \sqrt[4]{\frac{\sqrt{S^2-1}+\sqrt{2}}{\sqrt{S^2-1}-\sqrt{2}}},$$

and Z^* is complex conjugated to Z.

Equation (62) describes the Hopf bifurcation. Above the transition line, at $\Lambda > \Lambda_*$, the attractor of the dynamical system is a limit cycle with the radius proportional to $\sqrt{\Lambda-\Lambda_*}$, near

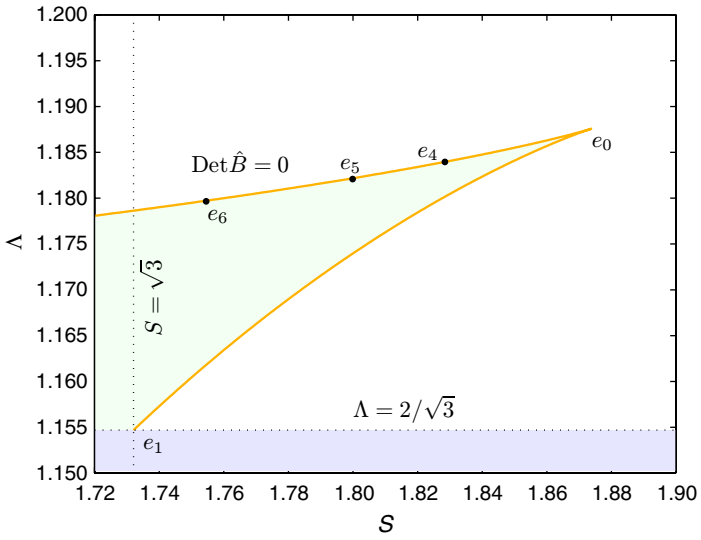

Figure 6. Phase diagram in the vicinity of the special point. Stability boundaries of the 'left' tank-treading regime.

the transition curve. This motion corresponds to trembling since the radius is small, and the limit cycle is not surrounding a pole, as can be seen from figure 3.

The parameters in equation (62) have a 'critical' dependence near the special point $S=\sqrt{3}$ and $\Lambda=2/\sqrt{3}$. In particular, the characteristic frequency of the bifurcation is proportional to $\sqrt{S-\sqrt{3}}$. However, surprisingly, the amplitudes of the Θ and Φ variations can be estimated as $\sqrt{\Lambda-\Lambda_*}$, without a 'critical' dependence on $S-\sqrt{3}$.

The vicinity of the special point e_1 needs an additional analysis since the frequency $\tau^{-1}\sqrt{S^2-3}$ of the Hopf bifurcation tends to zero as the point is approached and the approximation leading to equation (62) ceases to be valid there.

6.2. The tank-treading to tumbling transition

The tank-treading to tumbling transition is determined by the condition $\det\hat{B}=0$, where $\hat{B}$ is the stability matrix introduced by equation (60) for the symmetric solution. The corresponding transition curve on the S–Λ plane has a complicated shape. One obtains from equations (58) and (59) that the curve can be described as

$$S=\frac{\zeta^2\sqrt{15-32\zeta^2+16\zeta^4}}{1-\zeta^2},\qquad \Lambda=\frac{\sqrt{-8\zeta^4+12\zeta^2-3}}{\zeta^2\sqrt{5-4\zeta^2}},\tag{63}$$

where the parameter ζ varies from $1/\sqrt{2}$ to $\sqrt{3}/2$. Near the special point e_1 (where $S=\sqrt{3}$ and $\Lambda=2/\sqrt{3}$), the curve is presented in figure 6. The boundary value $\zeta=1/\sqrt{2}$ corresponds to the above special point e_1, and the boundary value $\zeta=\sqrt{3}/2$ corresponds to the point $S=0$ and $\Lambda=2/\sqrt{3}$. The expressions for S and Λ have a maximum at $\zeta_0=\sqrt{1-2^{-4/3}}$, $S\approx 1.8737-46.97(\zeta-\zeta_0)^2$ near the maximum. The value $\zeta=\zeta_0$ corresponds to the turning point e_0 in figure 6.

To be more precise, the condition $\det B=0$ determines the tank-treading decay point. Therefore the orange curve determines the stability boundaries of the tank-treading regime

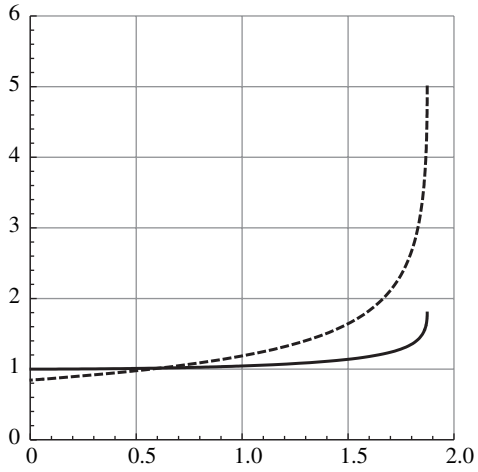

Figure 7. S-dependence of the parameters A (solid line) and B (dashed line).

obtained by continuation from the left region. Different parts of the curve correspond to different transformations. The segments e_1e_0 and e_0e_4 correspond to transition into the tank-treading regime obtained by continuation from the right region. Therefore there is a coexistence region of two tank-treading regimes. The segment e_4e_6 corresponds to transition into trembling. The point e_5, as we pointed out, corresponds to the termination point of the trembling instability curve. Therefore there exists a region of coexistence of the 'left' tank-treading and trembling. The residue of the curve, to the left of the point e_6, corresponds to the tank-treading to tumbling transition.

Let us consider the upper part of the orange curve in figure 6, which corresponds to the interval $\zeta_0 < \zeta < \sqrt{3}/2$ in equation (63). We are interested in the dynamics of the 'angles' Θ and Φ in the vicinity of the curve. There is a single degree of freedom possessing slow dynamics in the vicinity. The dynamics can be described in terms of an equation for Φ; the 'angle' Θ is adiabatically adjusted to the 'angle' Φ. The equation is

$$\tau\,\partial_t\delta\Phi = S\left[A\,\delta\Lambda + B\sqrt{S_0 - S}(\delta\Phi)^2\right], \tag{64}$$

where $\delta\Phi$ is a deviation of Φ from its stationary value taken at the transition curve at a given S and $\delta\Lambda = \Lambda - \Lambda(S)$. Here $\Lambda(S)$ is determined by equation (63), and A and B are functions of S plotted in figure 7. Note that the parameters have square-root singularities near $S = S_0$, where S_0 corresponds to the turning point, e_0 in figure 6.

The lower part of the orange curve, the segment e_0e_1 in figure 6, corresponds to the interval $1/\sqrt{2} < \zeta < \zeta_0$. As for the upper part of the curve, there exists a single soft degree of freedom in the vicinity of the segment. An equation for the degree of freedom can be written as

$$\tau\,\partial_t\delta\Phi = (S - \sqrt{3})\left[\tilde{A}\,\delta\Lambda + \tilde{B}\sqrt{S_0 - S}(\delta\Phi)^2\right], \tag{65}$$

analogously to equation (64). The parameters $\tilde{A}$ and $\tilde{B}$ in equation (65) are functions of S plotted in figure 8, and the meaning $S = \sqrt{3}$ corresponds to the special point e_1.

Equations (64) and (65) are characteristic of the saddle–node bifurcation. For equation (64), at $\delta\Lambda < 0$ (below the transition curve) there exists a stable stationary point $\delta\Phi \propto \sqrt{|\delta\Lambda|}$. It corresponds to the tank-treading regime. At $\delta\Lambda > 0$ (above the transition line) there are no

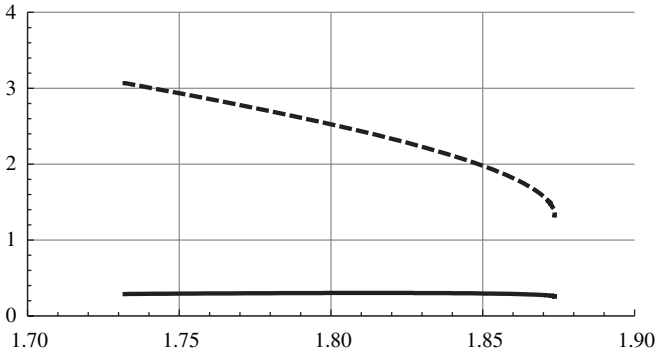

Figure 8. S-dependence of the parameters $\tilde{A}$ (solid line) and $\tilde{B}$ (dashed line).

stationary points described by equation (64). To establish the state of the system in this case, it is not enough to use equation (64) obtained by expanding over deviations of the 'angles' Θ and Φ. As our previous analysis shows, the instability occurring at $\delta\Lambda > 0$ can lead to tumbling, trembling or 'right' tank-treading. For equation (65), the sign of $\delta\Lambda$ should be changed: a stable stationary point exists above the curve at $\delta\Lambda > 0$. The instability developing below the curve at $\delta\Lambda < 0$ leads to the 'right' tank-treading.

As follows from equations (64) and (65), an additional slowdown of the dynamics can be observed near the turning point e_0. The functions B and $\tilde{B}$ have a finite limit as $S \to S_0$. To avoid a misunderstanding, note that the vesicle dynamics cannot be described in terms of equations (64) and (65) near the turning point where the factors in front of $(\delta\Phi)^2$ tend to zero and higher order terms of the expansion over the 'angle' deviations should be taken into account. The vesicle dynamics cannot be described in terms of equation (65) near the point e_1 as well, since the coefficients in the right-hand side of the equation tend to zero as one approaches this point. Its close vicinity needs a special consideration; the conclusion is the same as the one made in the previous subsection.

Note also that the case of weak flows, $S \ll 1$, requires an additional analysis since there are two soft degrees of freedom in the limit (corresponding to solid body motions of the equilibrium uniaxial ellipsoid), instead of the single degree of freedom described by equation (64). We postpone an analysis of the case to the next section.

6.3. Complete phase diagram

Collecting together all the results obtained above, one finds the complete phase diagram plotted in figure 9. The red line represents the tank-treading to trembling transition, whereas the orange line determines the tank-treading to tumbling transition. A transition line from tumbling to trembling, obtained numerically, is depicted by a dashed line in figure 9. We present the coexistence region of spinning and tumbling. We also plot in figure 9 the green line separating the damping and the oscillating relaxation modes in the tank-treading regime.

The tank-treading domain (containing stable stationary points) consists of the light violet strip below the line $\Lambda = 2/\sqrt{3}$ (where Φ is positive) and the light green sub-region above the line $\Lambda = 2/\sqrt{3}$ (where Φ is negative for $S > \sqrt{3}$). To avoid a misunderstanding, note that other stationary solutions of the system (58) and (59) exist in the domain $\Lambda > \sqrt{2}\sqrt{1 - 1/S^2}$, which are stable in terms of the variables Θ and Φ. However, a stability investigation in the framework

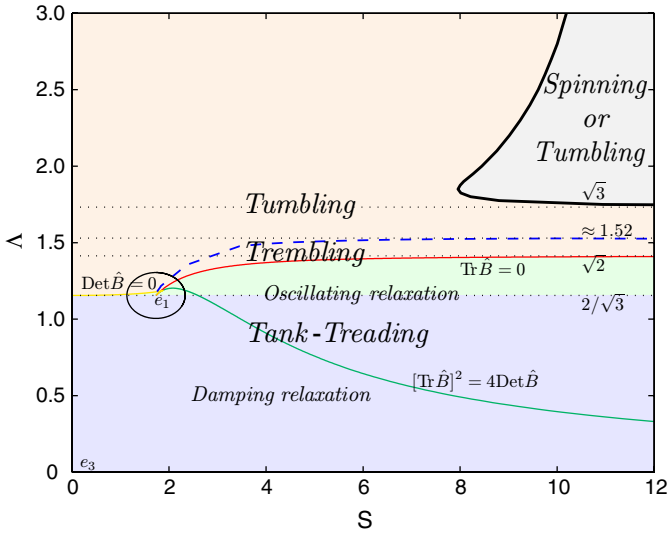

Figure 9. Complete phase diagram.

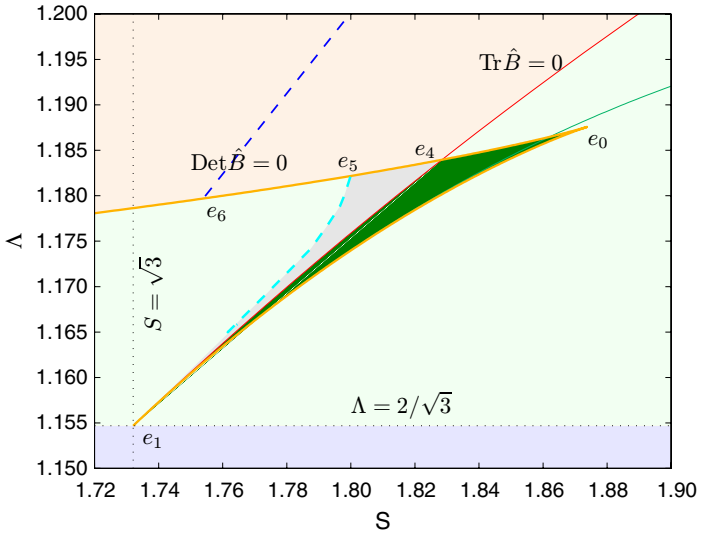

Figure 10. Phase diagram in the vicinity of the special point.

of the complete system of equations (54) shows that these solutions are unstable in the extended space (with the variables J and Ψ included). Therefore, these solutions cannot be realized as a tank-treading motion.

The phase diagram has a complicated structure near a special point $S=\sqrt{3}$, $\Lambda=2/\sqrt{3}$. A vicinity of the point is depicted in figure 10, where the regions of coexistence of two different stable points (green triangle) and of a stable point and of a limit cycle (fuchsia triangle) are shown. In other words, the green region in figure 10 corresponds to coexistence of two tank-treading regimes, whereas the fuchsia region in figure 10 corresponds to coexistence of the tank-treading and trembling regimes. The picture in figure 10 can be obtained as a combination of the pictures plotted in figures 5 and 6.

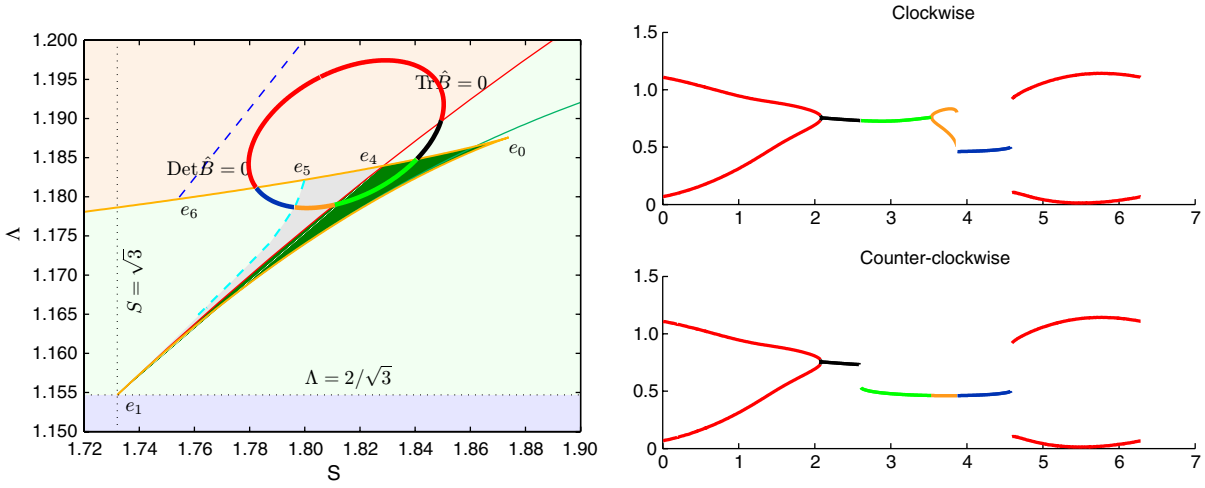

Figure 11. Θ angle in different dynamical regimes.

Different regimes of vesicle dynamics are illustrated in figure 11. In plotting the graphs, we assumed that the system parameters are adiabatically changed along the ellipse curve depicted on the left phase diagram. During this non-stationary process one observes different values of the angle Θ. In the red part of the curve, corresponding to the trembling regime the angle Θ oscillates within the boundaries shown on the right graph. Black and blue parts correspond to the tank-treading regime where the angle Θ is constant. Two tank-treading regimes coexist in the green region, and the vesicle relaxes to one of them depending on the initial condition. On the line $e_1 - e_4$ one of these tank-treading points bifurcates into the trembling cycle. Trembling and tank-treading regimes coexist in the orange part of the curve. Note that there is hysteresis in the system. The choice between coexisting regimes depends on the direction of the circuit. One can also see that there are two types of bifurcations between tank-treading and trembling regimes. The Hopf bifurcation is observed when passing the $e_1 - e_4$ line and the saddle–node one is observed when passing the $e_6 - e_5$ line.

7. Special cases

We established the general peculiarities of the vesicle dynamics in an external planar flow which appears to be rich in different types of behavior. The phase diagram depicted in figures 9 and 10 contains a great deal of domains and has a complicated structure. The situation is simplified for different limiting cases, which can be examined in more detail. Below, we present an analysis of some limit cases that seem to be primarily compared with experiment. Strong external flows are analyzed in a separate section.

7.1. Almost rotational flows and big viscosity contrast

Let us consider the case $\Lambda \gg 1$. The definition (50) reads that the limit $\Lambda \to \infty$ is achieved either at $\omega/s \to \infty$, where s and ω are the strain and the angular velocity of the external flow, see equation (5), or at $a \to \infty$, where a is the 'generalized viscosity contrast' (45). The case $\omega/s \to \infty$ corresponds to a purely rotational external flow, where the fluid rotates as a whole

with all inclusions. The case $a \to \infty$ corresponds to a solid body behavior of the vesicle, so one should reproduce the classical Jeffery's result [40], which predicts that for external flows with $\omega > \sqrt{\Delta}s$ the rigid ellipsoid is in the tumbling regime[3].

In accordance with this reasoning, we find from equation (54) that in the case $\Lambda \gg 1$ the vesicle rotates with the angular velocity ω of the external flow having a nearly equilibrium shape. Corrections to the equilibrium shape induced by the elongational part of the flow appear to be small due to averaging over the relatively fast rotation. Therefore in the main approximation the vesicle shape is the equilibrium one (52), where the angle ϕ grows linearly as time goes. And the question is to determine the angle ϑ between the principal ellipsoid semiaxis and the rotation axis Z.

The ϑ dynamics appears to be much slower than rotations with the frequency ω. To establish an equation for ϑ, one has to take into account small deviations of the 'angles' Θ, J, Φ and Ψ from their equilibrium values (52). The deviations are separated into terms oscillating with the frequency ω and approximately constant corrections induced by the oscillating terms. The oscillating terms and the corrections can be analyzed by expanding the equations (54). After that the equation for ϑ can be extracted, say, by averaging the equation (54) for J over the oscillations. A result of this bulky procedure is relatively simple:

$$\tau \partial_t \vartheta = \frac{\sin(2\vartheta)}{192\Lambda^2}\{12[7+\cos(2\vartheta)] - S^2[1+3\cos(2\vartheta)]\sin\vartheta\}. \tag{66}$$

To avoid a misunderstanding, note that the equation is correct provided $S \ll \Lambda$.

Tumbling and spinning correspond to stable stationary solutions of equation (66) that can be found by equating to zero the right-hand side of the equation. The solution $\vartheta = 0$ is always unstable. The solution $\vartheta = \pi/2$ is always stable; it corresponds to tumbling. If $S > S_{\rm bd}$,

$$S_{\rm bd} = \sqrt{\frac{78\sqrt{10}-120\sqrt{3}}{263\sqrt{10}-480\sqrt{3}}} \approx 11.48, \tag{67}$$

then there are two additional solutions, stable and unstable. The stable solution corresponds to spinning that, consequently, can be realized at $S > S_{\rm bd}$ for large $\Lambda \gg 1$. The value $S = S_{\rm bd}$ corresponds to the left boundary of the spinning domain in figure 4. The stationary value of the angle ϑ diminishes as S grows, it is $\arcsin\sqrt{4-2\sqrt{10}/\sqrt{3}}$ at $S = S_{\rm bd}$, and passes to $24/S^2$ at large S.

7.2. Purely elongational flow

The purely elongational flow corresponds to the case $\omega = 0$, that is, $\partial_y V_x = -\partial_x V_y = s$. Therefore, in our designations, the elongation is directed along the main diagonal in the X–Y plane.

The condition $\omega = 0$ leads to $\Lambda = 0$, in accordance with the definition (50). In this case, the system of equations (58) and (59) has a stable stationary point Φ_0, Θ_0, determined by the relations

$$\Phi_0 = \pi/4, \quad S\sin\Theta_0 = \cos(3\Theta_0). \tag{68}$$

[3] Note that the special limit $a \to \infty$ at fixed $\omega/s \ll \sqrt{\Delta}$ (leading to $\Lambda \to \infty$) needs special care, since it is not covered by equations (54) written in the main approximation in Δ. Although the vesicle behaves as a rigid body in this limit, it is in the tank-treading regime.

The 'angle' Θ_0 monotonically decreases from $\pi/6$ to zero as S increases from zero to infinity. The value $\Phi_0 = \pi/4$ is quite natural since it corresponds to the vesicle orientation along the elongation direction, as can be seen from equation (57). The stability check of the solution (68) shows that the point (68) is stable. In the limit $S \gg 1$, both 'angles' relax to their equilibrium values with the same rate $8\sqrt{10\pi}\, s(3\sqrt{3\Delta}\, a)^{-1}$.

Recently, a wrinkling phenomenon was observed in purely elongational flows at a sudden inversion of the elongation direction, see [45]. The effect can be explained in the framework of the theoretical scheme developed in our paper; the corresponding analysis is presented in [46].

7.3. Weak external flows

Let us consider weak external flows characterized by the condition $S \ll 1$. This case has been already discussed in section 3.3 from the phenomenological point of view. Here the case is analyzed in terms of the 'angles' Θ and Φ, enabling one to establish a value of the phenomenological constant D, introduced in equation (31).

As follows from equation (58), for $S \ll 1$ the 'angle' Θ is close to $\pi/6$, which is a stable point of the equation. Substituting the value $\Theta = \pi/6$ into equation (59), one obtains a closed equation for the 'angle' Φ

$$\tau\, \partial_t \Phi = (S/\sqrt{3}) \cos(2\Phi) - S\Lambda/2. \tag{69}$$

If $\Lambda \ll 2/\sqrt{3}$ then equation (69) has a stationary point

$$\Phi = \frac{1}{2} \arccos\left(\frac{\sqrt{3}\,\Lambda}{2}\right), \tag{70}$$

which is stable. For $\Lambda > 2/\sqrt{3}$ all the solutions correspond to indefinitely increasing $\Phi(t)$, that is, to the tumbling regime. Therefore $\Lambda = 2/\sqrt{3}$ is the transition point from tank-treading to tumbling.

For $\Theta = \pi/6$, the expression (57) describes a prolate uniaxial ellipsoid with the principal axis directed along the vector (32) with $\phi = \Phi$ and $\vartheta = 0$. Comparing then equation (69) with (33) (obtained for a shear flow with $s = \omega = \dot{\gamma}/2$), one finds

$$D = \frac{8\sqrt{10\pi}}{3a\sqrt{\Delta}}. \tag{71}$$

As it should be, the transition point $D = 1$ from tank-treading to tumbling corresponds to $\Lambda = 2/\sqrt{3}$. Let us stress that the value (71) does not depend on the character of the external flow. Therefore the equation (31) with the parameter (71) is correct for any weak external flow.

Note that in the 'rigid body' limit $a \to \infty$ (where the viscosity of the internal fluid or the membrane viscosity tends to infinity) the quantity (71) tends to zero. However, a description of higher-order terms in Δ shows that in the limit D stops to decrease and stabilizes at a value of the order of $\sqrt{\Delta}$. The reduction of D leads to a solid rotation of the vesicle in the particular case of the external shear flow as follows from equations (33) and (34). The behavior corresponds to the classical result of Jeffery [40], who demonstrated that a solid ellipsoid rotates in an external planar flow, provided $\omega > \sqrt{\Delta} s$.

8. Strong external flows

Here we analyze the case of strong external planar flows, defined by the inequality $S \gg 1$, in our designations. In this case the leading role in determining the vesicle shape and its dynamics is played by the external flow. However, surprisingly, the vesicle bending rigidity cannot be neglected even in this limit case. Moreover, our scheme, where the rigidity is taken into account, appears to be applicable even in the case of extremely strong flows, $S \gg 1/\sqrt{\Delta}$.

8.1. Truncated equations

In the case of strong external flows, where S is large, the last term in the right-hand side of equation (54) is small in comparison with the first one. After neglecting the term, one arrives at the following system of equations written in terms of the 'angles' introduced by equation (51):

$$(\tau/S)\,\partial_t\Theta = -\sin\Theta\sin(2\Phi), \qquad (\tau/S)\,\partial_t\Phi = \frac{1}{2}\left[\frac{\cos(2\Phi)}{\cos\Theta} - \Lambda\right],$$
$$(\tau/S)\,\partial_t\Psi = \Lambda/2, \qquad \partial_t J = 0. \tag{72}$$

The system (72) corresponds to the limit case considered by Misbah [8] and then by Vlahovska and Gracia [25]. In this subsection, we analyze solutions of the system (72). Their relation to an observable vesicle behavior is not straightforward and is discussed in the next subsection.

The system of equations (72) has two integrals of motion: J and an additional integral, Υ, which can be introduced via the relation

$$\frac{\sin\Upsilon}{\Lambda - \cos\Upsilon} = \frac{\sin\Theta}{\Lambda - \cos\Theta\cos(2\Phi)}. \tag{73}$$

To specify Υ unambiguously, we choose a root of the equation (73) lying in the domain $|\Upsilon| < \arccos(1/\Lambda)$. Existence of the integrals of motion implies that the character of the vesicle evolution, described by the system of equations (72), depends on initial conditions (that determine values of the integrals).

The system of equations (72) can be completely integrated. For this purpose, we introduce a variable

$$\rho = \exp\left\{(S/\tau)\int_0^t \mathrm{d}t'\,\cos[\Theta(t')]\sin[2\Phi(t')]\right\}. \tag{74}$$

It is convenient to choose an initial time, as a moment, when $\Phi = 0$ and $|\Theta| < \arccos(1/\Lambda)$ (such a time exists for arbitrary initial conditions). Then the initial conditions turn to $\rho = 1$ and $\partial_t\rho = 0$, and one derives from the system (72) the following equation:

$$(\tau/S)^2\,\partial_t^2\rho = -(\Lambda^2 - 1)\rho + \Lambda^2 - \Lambda\cos\Upsilon, \tag{75}$$

which can be obviously solved explicitly. The parameters Φ and Θ are expressed, via the variables ρ and Υ, as

$$\cos\Theta\cos(2\Phi) = \Lambda - (\Lambda - \cos\Upsilon)/\rho, \tag{76}$$

$$\cos\Theta\sin(2\Phi) = (\tau/S)\partial_t\rho/\rho. \tag{77}$$

A solution of equation (75) behaves differently at $\Lambda < 1$ and at $\Lambda > 1$. If $\Lambda < 1$, then the variable ρ goes exponentially to infinity as time grows; thus the right-hand sides of the equations (76) and (77) tend to constants giving the stationary point $\Theta = 0, 2\Phi = \arccos\Lambda$. Thus, we

arrive at the tank-treading regime. If $\Lambda > 1$, then the variable ρ experiences oscillations. Therefore the vesicle dynamics corresponds to some closed trajectory in the Θ–Φ plane which is determined by the values of J and Υ. If the angle Φ grows (decreases) indefinitely, so that the poles $\Theta = \pm\pi/2$ are inside the trajectory, the vesicle is in the tumbling regime. Otherwise, if the oscillations of Φ are bounded the dynamics corresponds to trembling.

For the truncated system (72) the tumbling and trembling regimes coexist for any $\Lambda > 1$. A choice between the regimes is determined by a value of Υ. If $\cos\Upsilon > 2\Lambda/(\Lambda^2+1)$, then the closed trajectory corresponds to tumbling; otherwise the cycle corresponds to trembling. If Υ takes one of its boundary values, that is, if $\cos\Upsilon = 1/\Lambda$, then the trajectory degenerates into a single point with

$$\Phi = 0, \qquad \cos\Theta = 1/\Lambda. \tag{78}$$

Thus, even at $\Lambda > 1$ the truncated system of equations (72) has two stationary points corresponding to the tank-treading regime.

8.2. Slow dynamics

We demonstrated that the truncated system of equations (72) can be completely integrated. However, the system cannot be directly used for the analysis of the vesicle dynamics in the limit of strong flows $S \gg 1$. Indeed, the type of solution of the system depends strongly on initial conditions and admits different closed trajectories for any $\Lambda > 1$. Both these properties contradict obviously the general properties of dissipative dynamics and the results obtained in section 5.1. The contradiction is resolved if one restores the terms omitted in the truncated system (72) and originating from the last (nonlinear in U) term in the right-hand side of equation (54). The restored (κ-proportional) term modifies the vesicle dynamics, leading to a relatively slow evolution of both integrals of motion, J and Υ, that produces a well-defined behavior, independent of the initial conditions.

Below, we consider the case $\Lambda > 1$ where the truncated system of equations (72) leads to limit cycles. Then, considering solutions of the complete system of equations, one can separate fast motion along the closed trajectories and relatively slow evolution of the (approximate) integrals of motion on timescales larger than the cycle period. Note that a typical timescale associated with the fast dynamics is τ/S, whereas a typical time of the slow dynamics is τ. The large ratio of the times justifies the separation. The equation controlling the slow evolution can be found by averaging over the trajectory period of the expressions for the time derivatives of J and Υ obtained from the complete system (54). For this averaging, one can use the fast dynamics described by the system (72). The result can be symbolically written as

$$\tau\,\partial_t\Upsilon = \dot{\Upsilon}, \qquad \tau\,\partial_t J = \dot{J}, \tag{79}$$

where $\dot{\Upsilon}$ and $\dot{J}$ are some functions of Υ, J and Λ.

The dynamical equations (79) have stationary points, which can be found from the conditions $\dot{\Upsilon} = 0$ and $\dot{J} = 0$. The expression for $\dot{J}$ is antisymmetric in J as a consequence of the initial symmetry of the dynamic equations under the reflection $z \to -z$ (or $\theta \to -\theta$). Therefore there are stationary points with $J = 0$, corresponding to a symmetric vesicle shape.

In the case $J = 0$, one finds from equations (58), (59) and (73) that $\dot{\Upsilon} = \langle(\partial\Upsilon/\partial\Theta)\cos(3\Theta)\rangle$, where angular brackets mean averaging over the period. Calculating the

average, one obtains

$$\dot{\Upsilon} = \frac{\Lambda(\Lambda\cos\Upsilon - 1)}{\Lambda^2 - 1}\left[1 - \frac{4|\mathfrak{U}|\left(\Lambda^2 - 1\right)^{3/2}}{\Lambda\left(\mathfrak{U}^2 + 1\right)^{3/2}}\right], \tag{80}$$

where $\mathfrak{U} = (\Lambda - \cos\Upsilon)\csc\Upsilon$. Note that the expression (80) is symmetric in Υ. It is a consequence of the equations (72) and the relation (73) that leads to the conclusion that at $\Upsilon \to -\Upsilon$ the solution transforms as $\Theta \to -\Theta$ and $\Phi \to \Phi$. Therefore an average of any even function of Θ, like $\dot{\Upsilon}$, should be even in Υ.

The stationary points with $J = 0$ can be found by equating the expression (80) to zero. If $1 < \Lambda < \sqrt{2}$ then there are two stationary points, $\Upsilon = \arccos(1/\Lambda)$ and $\Upsilon = -\arccos(1/\Lambda)$. The situation corresponds to tank-treading. The first stationary point is stable and gives the solution (78), the second one is unstable. If $\Lambda > \sqrt{2}$, then the stationary points $\Upsilon = \pm\arccos(1/\Lambda)$ survive but become unstable (the point $\Upsilon = -\arccos(1/\Lambda)$ is unstable under fluctuations with nonzero J). Besides at $\Lambda > \sqrt{2}$ there appears a new pair of stationary points $\Upsilon = \pm\Upsilon_0$, where Υ_0 can be found by equating to zero the expression in square brackets in equation (80). The positive solution, $\Upsilon = \Upsilon_0$, is stable, whereas the negative solution, $\Upsilon = -\Upsilon_0$, appears to be unstable. The solution $\Upsilon = \Upsilon_0$ corresponds either to trembling or tumbling, depending on Λ. A numerical investigation based on the expression (80) shows that the boundary value of Υ is achieved at $\Lambda \approx 1.52$, the region $\Lambda > 1.52$ corresponds to tumbling, whereas the region $\Lambda < 1.52$ corresponds to trembling.

If $\Lambda \gg \sqrt{3}$, then there exists an additional stationary point of the equations (79) where

$$J = (1/2)\arccos((\Lambda^2 - 4)/(\Lambda^2 - 1)) \tag{81}$$

and $\Upsilon = -\arccos(1/\Lambda)$. The solution corresponds to the spinning regime that we discussed in subsection 5.3. The value $\Lambda = \sqrt{3}$ determines the asymptotic (at large S) behavior of the boundary of the spinning domain plotted in figure 4.

The above results are in agreement with the general analysis of section 5.

8.3. Extremely strong flows

The analysis made in the previous subsections is, strictly speaking, correct only for the flows with $S \lesssim 1/\sqrt{\Delta}$. For stronger flows, our consideration should be extended. Some additional terms of the higher order in u should be taken into account in the equation for u, which for $1/\sqrt{\Delta} \lesssim S$ are larger than those kept in equation (47). Leading corrections of such a kind can be estimated as su. They appear after accounting for the deviations of the vesicle shape from a spherical one while solving the Stokes equation for the internal and external problems. The corrections are associated with the contribution $\boldsymbol{v}^{(s)}$ to the membrane velocity, whereas the second term in the right-hand side of equation (47) is associated with the contribution $\boldsymbol{v}^{(\kappa)}$ to the membrane velocity, see equation (15). Such corrections are discussed in [27].

There is an essential difference between the terms $\boldsymbol{v}^{(s)}$ and $\boldsymbol{v}^{(\kappa)}$. If the term $\boldsymbol{v}^{(\kappa)}$ is neglected, then the equations possess an additional symmetry, they are invariant under the simultaneous time and space inversions, see subsection 2.3. Since the axes of our reference system are attached to the eigenvectors of the strain matrix $\hat{s}$, the space inversion is equivalent to the transformation $\varphi \to -\varphi$ and $\theta \to \theta$, that is, it can be written as $\Phi \to -\Phi$, $\Psi \to -\Psi$, $\Theta \to \Theta$ and $J \to J$ in terms of the 'angles' (51). Therefore the equations for the 'angles' should be invariant under the transformation

$$t \to -t, \quad \Phi \to -\Phi, \quad \Theta \to \Theta, \quad \Psi \to -\Psi, \quad J \to J, \tag{82}$$

if the membrane bending rigidity is neglected. One can easily check that the truncated equations (72) are invariant under the transformation (82), indeed. However, our analysis demonstrated that the symmetry is preserved even if higher in u terms will be taken into account provided $\kappa \to 0$.

If the corrections of the order of su to the truncated equation (72) are taken into account, the system of limit cycles, which are characteristics of this equation at $\Lambda > 1$, does not change its topology due to the small perturbations. In this case one can derive the equation for the slow dynamics of the quantity Υ, like in the previous subsection. Since $\Upsilon \to \Upsilon$ under the transformation (82), the resulting dynamic equations for Υ averaged over the cycle will be $\partial_t \Upsilon = 0$. Thus the corrections do not destroy the conservation of Υ. Analogously, one can demonstrate that the corrections cannot destroy the condition $J = 0$ since they lead to the averaged equation $\partial_t J = 0$.

Thus the corrections related to the s-proportional terms in the equation for u slightly disturb the limit cycles but do not destroy the conservation laws of the integral of motion. Consequently, the κ-proportional term should be taken into account to fix the values of the integrals. And we just found the leading κ-proportional term. It produces a selection leading to stable limit cycles or to stable stationary points. Since the selection is produced among limit cycles slightly disturbed in comparison with the ones corresponding to the truncated equation (72), the results will be the same in the main approximation in Δ. Therefore, the above results obtained for strong flows can be immediately extended to the extremely strong flows, where $S \gg 1/\sqrt{\Delta}$.

9. Conclusion

We have investigated the dynamics of nearly spherical vesicles in an external stationary flow, focusing mainly on the shear flow. Our calculation scheme is based on solving the $3d$ hydrodynamic (Stokes) equation with boundary conditions posed on the membrane. We accounted for both the membrane bending elasticity as well as the internal membrane viscosity, the latter leading to an additional dissipation mechanism. We have demonstrated that the system can be characterized by two dimensionless parameters that are combinations of the vesicle characteristics and of the external flow velocity derivatives.

One of the most interesting phenomena in the vesicle dynamics is a transition from the tank-treading regime to a regime where the vesicle shape changes in time. The latter occurs at relatively large viscosity contrast or a large rotational component of the external flow. We have demonstrated that in relatively weak flows direct transition from tank-treading to tumbling occurs, whereas in relatively strong flows one observes an intermediate regime, trembling. This behavior is in agreement with experiments by Kantsler and Steinberg [7] and numerical simulations by Noguchi and Gompper [9]. We have also predicted a new regime, spinning, that has to be observed in strong external flows. In the spinning regime, which coexists with tumbling, the vesicle shape varies in time in a complicated manner, resembling precession.

The possibility of an intermediate regime between tank-treading and tumbling was discussed theoretically, first by Misbah [8] and then (qualitatively) by Noguchi and Gompper [9]. Note, however, that the computational scheme that was used by Misbah [8] and then improved by Vlahovska and Gracia [25] is not self-consistent even though formally the authors have accounted for the leading terms of the equation for the vesicle distortions in strong external flows. This scheme leads to a strong dependence of the vesicle dynamics on initial

conditions and should therefore be improved by including higher-order terms, as was done in our work.

The impact of the high-order terms on the vesicle dynamics was also studied in [27] from the perspective of vesicle solutions rheology. The authors considered the same physical situation as the one investigated in our work, and the perturbation scheme developed in [27] is methodologically similar to the one described in our paper. Keeping the second-order angular harmonic they perform an expansion up to the third order in $\sqrt{\Delta}$ in the dynamical equation. As a result, Danker *et al* [27] reproduced our equation published in [26] up to the terms of order $S\sqrt{\Delta}$ (in our designations). In section 8, we have demonstrated that these corrections lead to a vanishingly small shift of the phase diagram transition lines, provided Δ is small. As is seen from the phase diagram presented in [27], even for $\Delta = 1$ the shift is not critical. Therefore our conclusions concerning two dimensionless parameters controlling the vesicle dynamics are correct, contrary to an assertion made in [27].

We demonstrated that the tank-treading to tumbling and the tank-treading to trembling transitions are essentially different. The first transition is described as a saddle–node bifurcation, whereas the second one is described as a Hopf bifurcation. We found the 'soft' degrees of freedom responsible for the transitions. Our theory predicts the existence of a special point on the phase diagram where the above two transition lines merge. One expects an essential 'critical' slowness of the vesicle dynamics near the point. In our work we derived the power laws describing the slowness.

A phenomenon recently discovered experimentally by Kantsler *et al* [45] is worth mentioning. It was observed that the relaxational dynamics of a vesicle in an external elongational flow is accompanied by the formation of wrinkles on a membrane at an abrupt change of the elongational direction. A theoretical explanation of this effect based on the approach developed in this paper was presented in [46]. It was shown there that the wrinkle formation is related to the dynamical instability provoked by the negative induced surface tension of the membrane.

We have investigated nearly spherical vesicles assuming that the excess area factor Δ is small. This allows one to formulate a powerful calculation procedure, enabling one to study the vesicle dynamics in detail analytically. However, the scheme based on the Stokes equation and correct boundary conditions at the membrane can be developed for a vesicle with arbitrary excess area.

We believe that the qualitative results of our theory are valid for vesicles with arbitrary excess area. Indeed, it is natural to expect that the character of the tank-treading regime destruction is different in weak and strong flows. Therefore for the region where the transition lines merge one should observe an extra slowdown of the vesicle dynamics. We also believe that the spinning regime is characteristic for vesicles with arbitrary excess area.

One should be somewhat careful in comparing an experiment with the phase diagram obtained in our work since the diagram is deduced ignoring thermal fluctuations. They play a relatively small role in the physics of membranes, since the bending module κ appears to be much larger than temperature. However, in the narrow vicinities of the tank-treading to tumbling transition and of the tank-treading to trembling transition, thermal fluctuation effects are relevant. The effects, which can be examined in the spirit of the works [47, 50, 51], constitute a subject of special investigation, to be done separately.

A natural application area of our results is dilute vesicle solutions. We believe that two features of our theory, the slowdown near the transition lines (and especially near their merging

point) and the tumbling–spinning bistability, can strongly influence rheological properties of the solutions. This will be a subject of future research.

Acknowledgments

We thank V Kantsler, I Kolokolov and V Steinberg for numerous valuable discussions. KT thanks Margo Levine for help in improving the manuscript. This work has been partially supported by RINKCE NSh-4930.2008.2, RFBR grant 06-02-17408-a and joint RFBR–Israel grant 06-02-72028. KT and SV acknowledge financial support from the 'Dynasty' and RSSF foundations. The work of KT was also supported in part by the NSF MRSEC Program under Award Number DMR-0213745.

References

[1] De Haas K H, Blom C, Van D E, Duits M H G and Mellema J 1997 *Phys. Rev.* E **56** 7132
[2] Shahidzadeh N, Bonn D, Aguerre-Chariol O and Meunier J 1998 *Phys. Rev. Lett.* **81** 4268
[3] Abkarian M, Lartigue C and Viallat A 2002 *Phys. Rev. Lett.* **88** 068103
[4] Abkarian M and Viallat A 2005 *Biophys. J.* **89** 1055–66
[5] Kantsler V and Steinberg V 2005 *Phys. Rev. Lett.* **95** 258101
[6] Mader M A, Vitkova V, Abkarian M, Viallat A and Podgorski T 2006 *Eur. Phys. J.* E **19** 389
[7] Kantsler V and Steinberg V 2006 *Phys. Rev. Lett.* **96** 036001
[8] Misbah C 2006 *Phys. Rev. Lett.* **96** 028104
[9] Noguchi H and Gompper G 2007 *Phys. Rev. Lett.* **98** 128103
[10] Kraus M, Wintz W, Seifert U and Lipowsky R 1996 *Phys. Rev. Lett.* **77** 3685
[11] Sukumaran S and Seifert U 2001 *Phys. Rev.* E **64** 011916
[12] Noguchi H and Takasu M 2002 *Phys. Rev.* E **65** 051907
[13] Noguchi H and Gompper G 2004 *Phys. Rev. Lett.* **93** 258102
[14] Noguchi H and Gompper G 2005 *J. Phys.: Condens. Matter* **17** S3439
[15] Noguchi H and Gompper G 2005 *Proc. Natl Acad. Sci. USA* **102** 14159–64
[16] Noguchi H and Gompper G 2005 *Phys. Rev.* E **72** 011901
[17] Biben T and Misbah C 2002 *Eur. Phys. J.* B **29** 311
[18] Biben T and Misbah C 2003 *Phys. Rev.* E **67** 031908
[19] Beaucourt J, Rioual F, Seon T, Biben T and Misbah C 2004 *Phys. Rev.* E **69** 011906
[20] Biben T, Kassner K and Misbah C 2005 *Phys. Rev.* E **72** 041921
[21] Keller S R and Skalak R 1982 *J. Fluid Mech.* **120** 27
[22] Rioual F, Biben T and Misbah C 2004 *Phys. Rev.* E **69** 061914
[23] Seifert U 1999 *Eur. Phys. J.* B **8** 405
[24] Olla P 2000 *Physica* A **278** 87–106
[25] Vlahovska P M and Gracia R S 2007 *Phys. Rev.* E **75** 016313
[26] Lebedev V V, Turitsyn K S and Vergeles S S 2007 *Phys. Rev. Lett.* **99** 218101
[27] Danker G, Biben Th, Podgorski Th, Verdier C and Misbah Th 2007 *Phys. Rev.* E **76** 041905
[28] Meuner J, Langevin D and Boccara N (ed) 1987 *Physics of Amphiphilic Layers* (*Springer Proc. in Physics* vol 21) (Berlin: Springer)
[29] Safran S A and Clark N A 1987 *Physics of Complex and Supermolecular Fluids* (New York: Wiley)
[30] Nelson D, Pvian T and Weinberg S 1989 *Statistical Mechanics of Membranes and Surfaces* (New York: World Scientific)
[31] Bellocq A M *et al* 1984 *Adv. Colloid Interface Sci.* **20** 167
[32] Porte G *et al* 1991 *Physica* A **176** 168

[33] Porte G *et al* 1992 *J. Physique* II **4** 8649
[34] Safran S A 1994 Statistical thermodynamics of surfaces, interfaces, and membranes *Front. Phys.* **90**
[35] Dimova R, Pouligny B and Dietrich C 2000 *Biophys. J.* **79** 340
[36] Canham P B 1970 *J. Theor. Biol.* **26** 61
[37] Helfrich W 1973 *Z. Naturf.* A **28c** 693
[38] Evans E 1974 *Biophys. J.* **14** 923
[39] Helfrich W 1975 *Z. Naturf.* B **103** 67
[40] Jeffery G B 1922 *Proc. R. Soc.* A **102** 161–79
[41] Lebedev V V and Muratov A R 1989 Dynamics of micelles and vesicles *Zh. Eksp. Teor. Fiz.* **95** 1751
Lebedev V V and Muratov A R 1989 *Sov. Phys.—JETP* **68** 1011 (Engl. Transl.)
[42] Kats E I and Lebedev V V 1993 *Fluctuational Effects in the Dynamics of Liquid Crystals* (New York: Springer)
[43] Zong-Can O-Y and Helfrich W 1989 *Phys. Rev.* A **39** 5280
[44] Juelicher F, Seifert U and Lipowsky R 1993 *Phys. Rev. Lett.* **71** 452
[45] Kantsler V, Segre E and Steinberg V 2007 *Phys. Rev. Lett.* **99** 178102
[46] Turitsyn K S and Vergeles S S 2008 *Phys. Rev. Lett.* **100** 028103
[47] Chertkov M, Kolokolov I, Lebedev V and Turitsyn K 2005 *J. Fluid. Mech.* **531** 251
[48] Lamb H 1932 *Hydrodynamics* 6th edn (Cambridge: Cambridge University Press)
[49] Happel J and Brenner H 1965 *Low Reynolds Number Hydrodynamics* (Englewood Cliffs, NJ: Prentice-Hall)
[50] Kats E I, Lebedev V V and Muratov A R 1996 *Pis. Zh. Eksp. Teor. Fiz.* **63** 203
Kats E I, Lebedev V V and Muratov A R 1996 *JETP Lett.* **63** 216 (Engl. Transl.)
[51] Turitsyn K S 2007 *Zh. Eksp. Teor. Fiz.* **132** 746
Turitsyn K S 2007 *JETP* **105** 655 (Engl. Transl.)